Fast Radio Burst Breakouts from Magnetar Burst Fireballs

Kunihito Ioka (YITP, Kyoto U.)

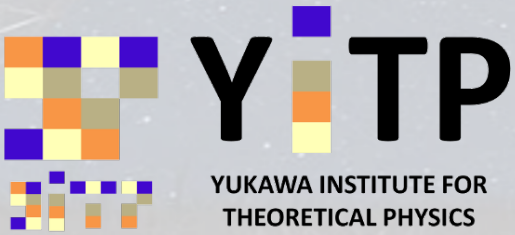

Fast Radio Bursts

Enigmatic transients

Extremely high $T_B \sim 10^{32\text{-}36}$K

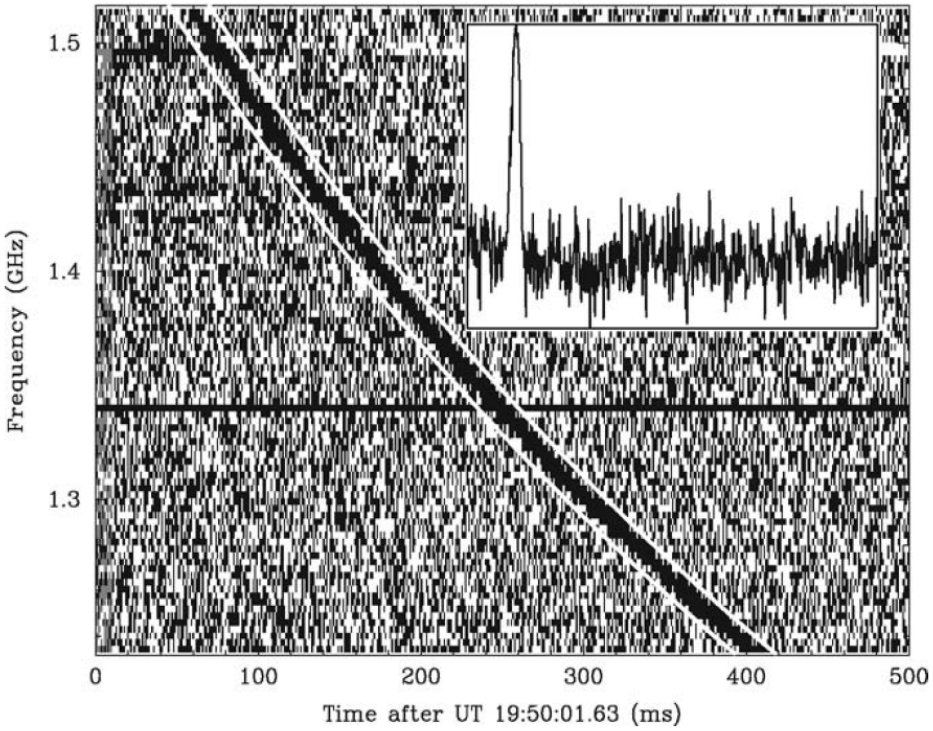

Lorimer+ 07
Thornton+ 13

FRB cosmology

DM as a unique probe

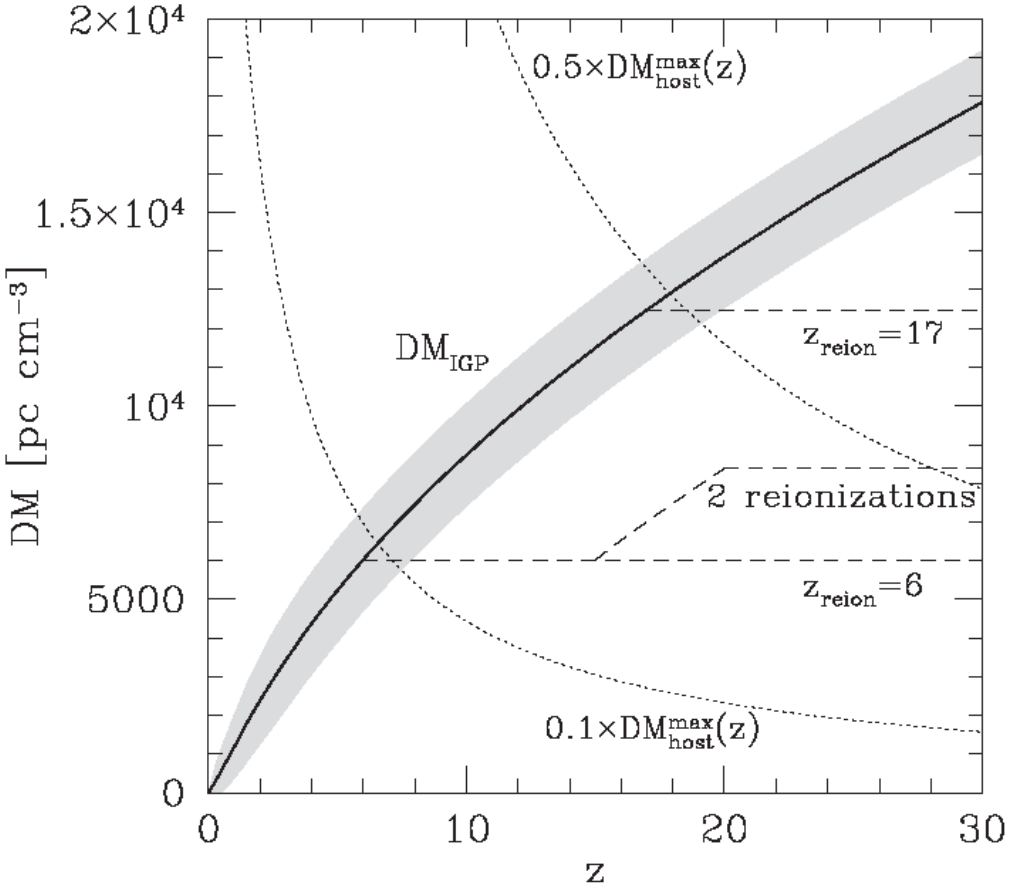

KI 03, Inoue 04

Macquart+ 20

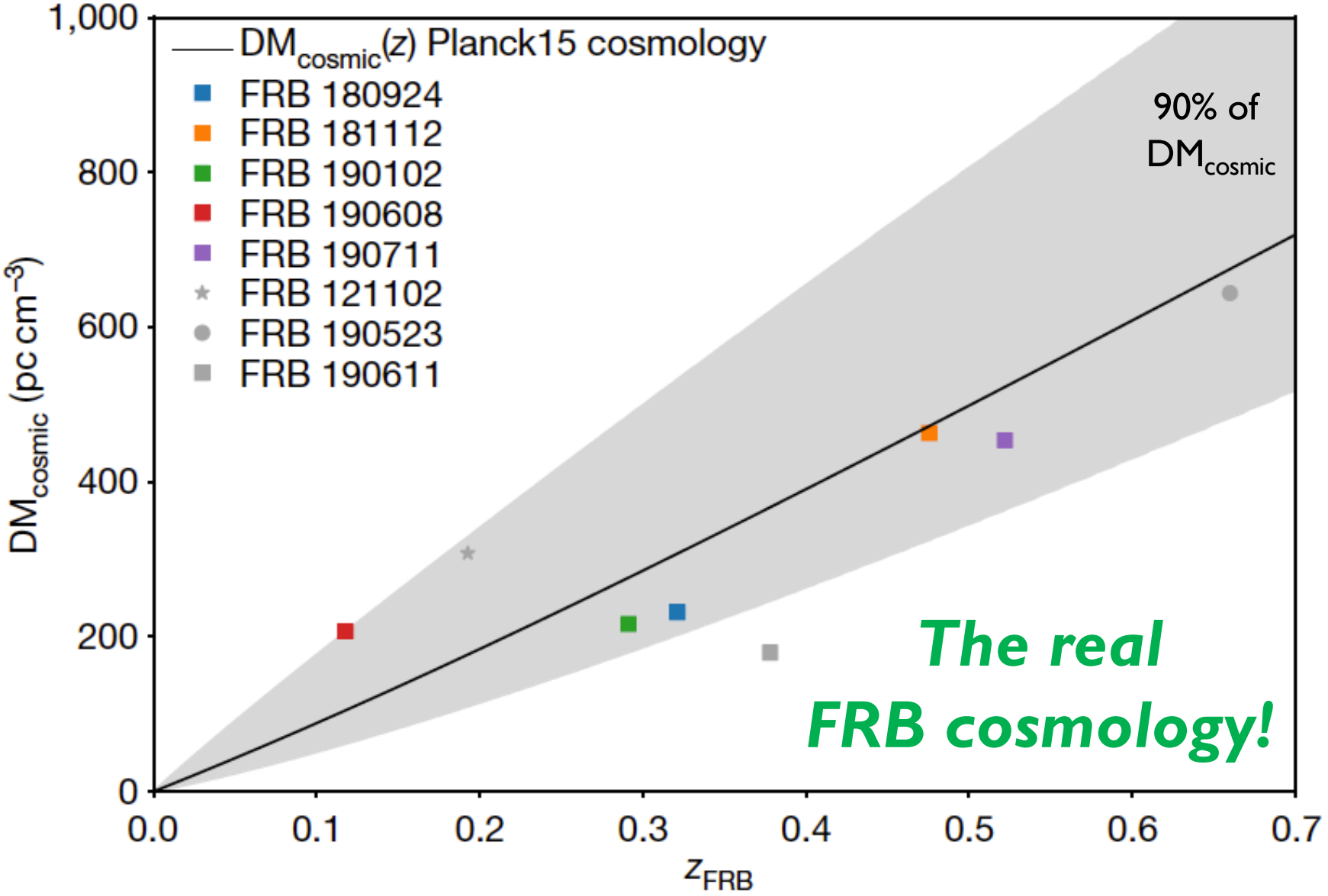
1,000
800
600
400
200
0
0.0
0.1
0.2
0.3
0.4
0.5
0.6
0.7
DM_{cosmic} (pc cm^{-3})
z_{FRB}
$DM_{cosmic}(z)$ Planck15 cosmology
FRB 180924
FRB 181112
FRB 190102
FRB 190608
FRB 190711
FRB 121102
FRB 190523
FRB 190611
90% of DM_{cosmic}
The real FRB cosmology!

Galactic FRB from Magnetar Bursts

A smoking gun! But new puzzles arise

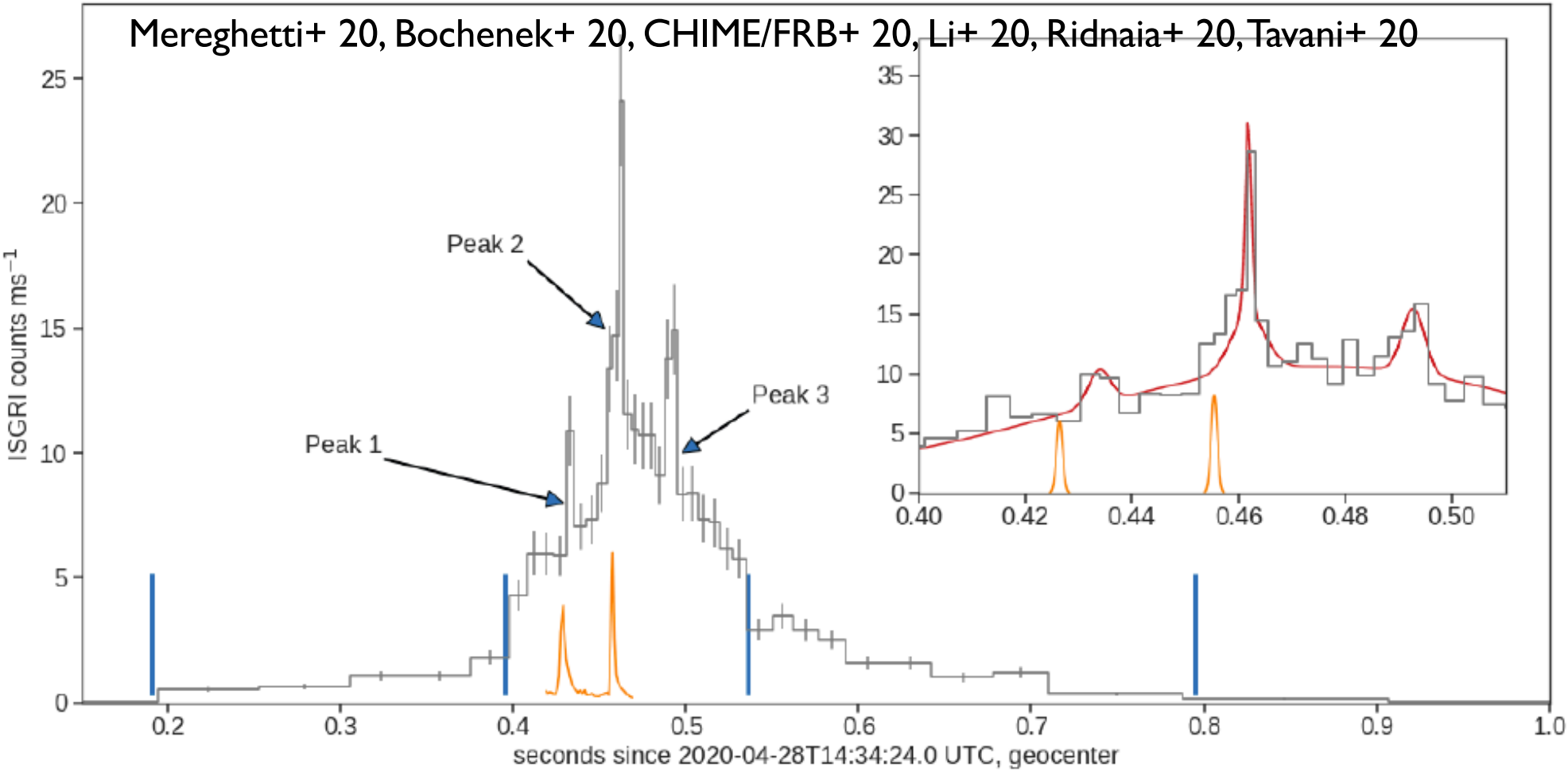

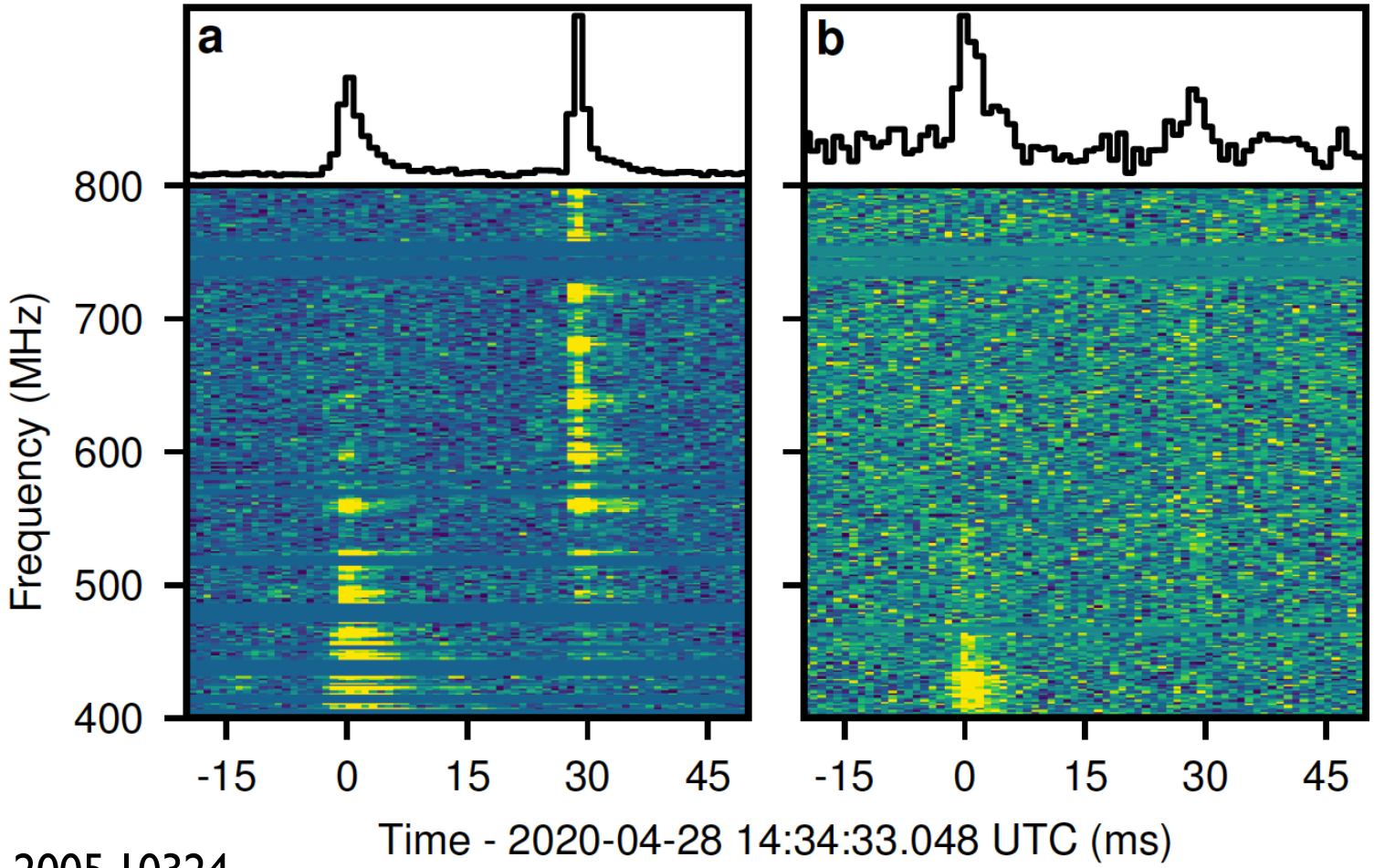

CHIME+ 2005.10324

The Algonquin Radio Observatory (ARO)

Figure 1: **Burst waterfalls.** Total intensity normalized dynamic spectra and band-averaged time-series (referenced to the geocentre) of the detections by (a) CHIME/FRB and (b) ARO, relative to the geocentric best-fit arrival time of the first sub-burst based on CHIME/FRB data. For CHIME/FRB, the highest S/N beam detection is shown. Dynamic spectra are displayed at 0.98304-ms and 1.5625-MHz resolution, with intensity values capped at the 1st and 99th percentiles. Frequency channels masked due to radio frequency interference are replaced with the median value of the off-burst region. The CHIME/FRB bursts show a "comb-like" spectral structure due to their detection in a beam sidelobe as well as dispersed spectral leakage that has an instrumental origin (see Methods).

STARE2 FRB

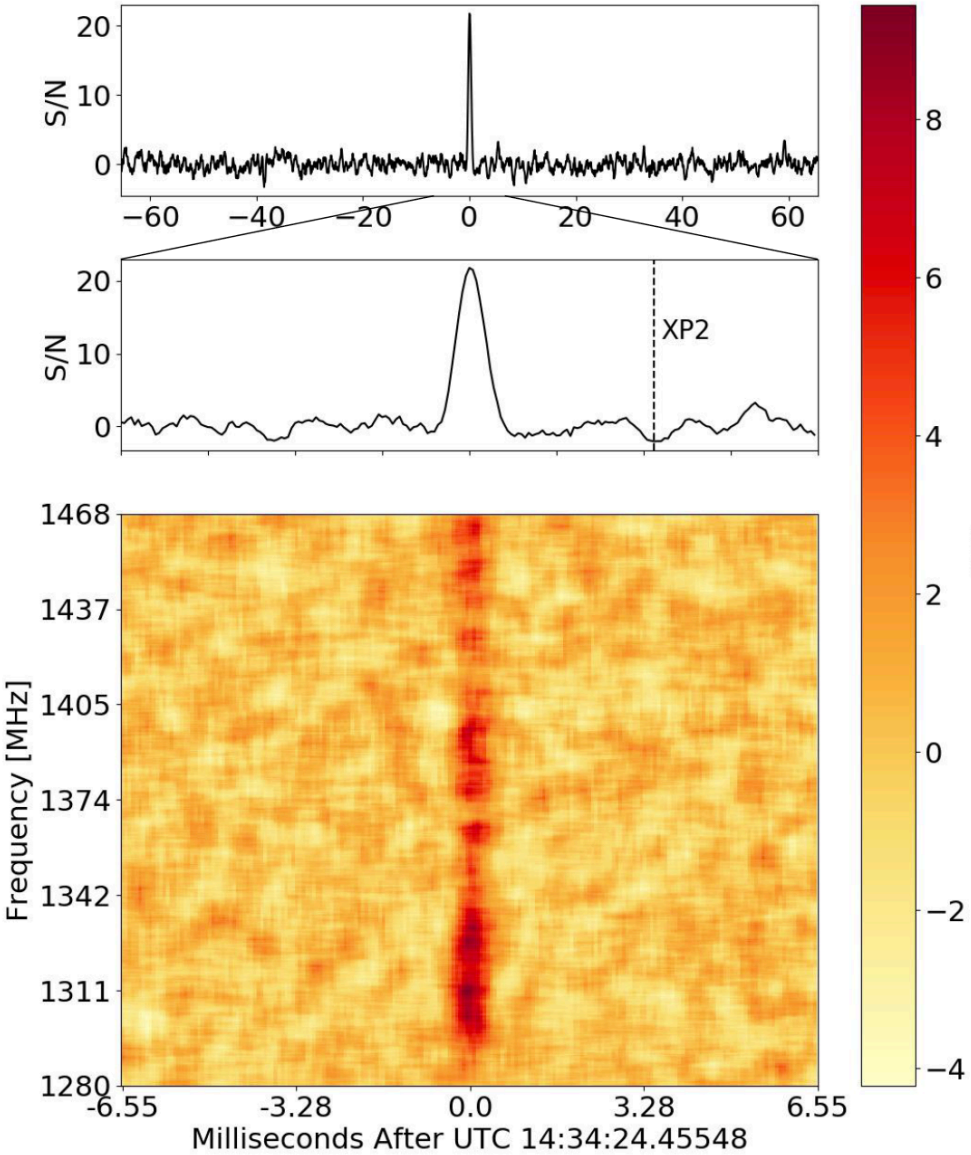

Owens Valley Radio Observatory alone

De-dispersed time series

DM=332.702 pc cm^{-3}

No other burst in a window of 131.072 ms

< 400 kJy ms

XP2: the second peak in X-ray

CHIME first reported kJy ms

STARE2 daily manual inspection

Bochenek+ 2005.10828

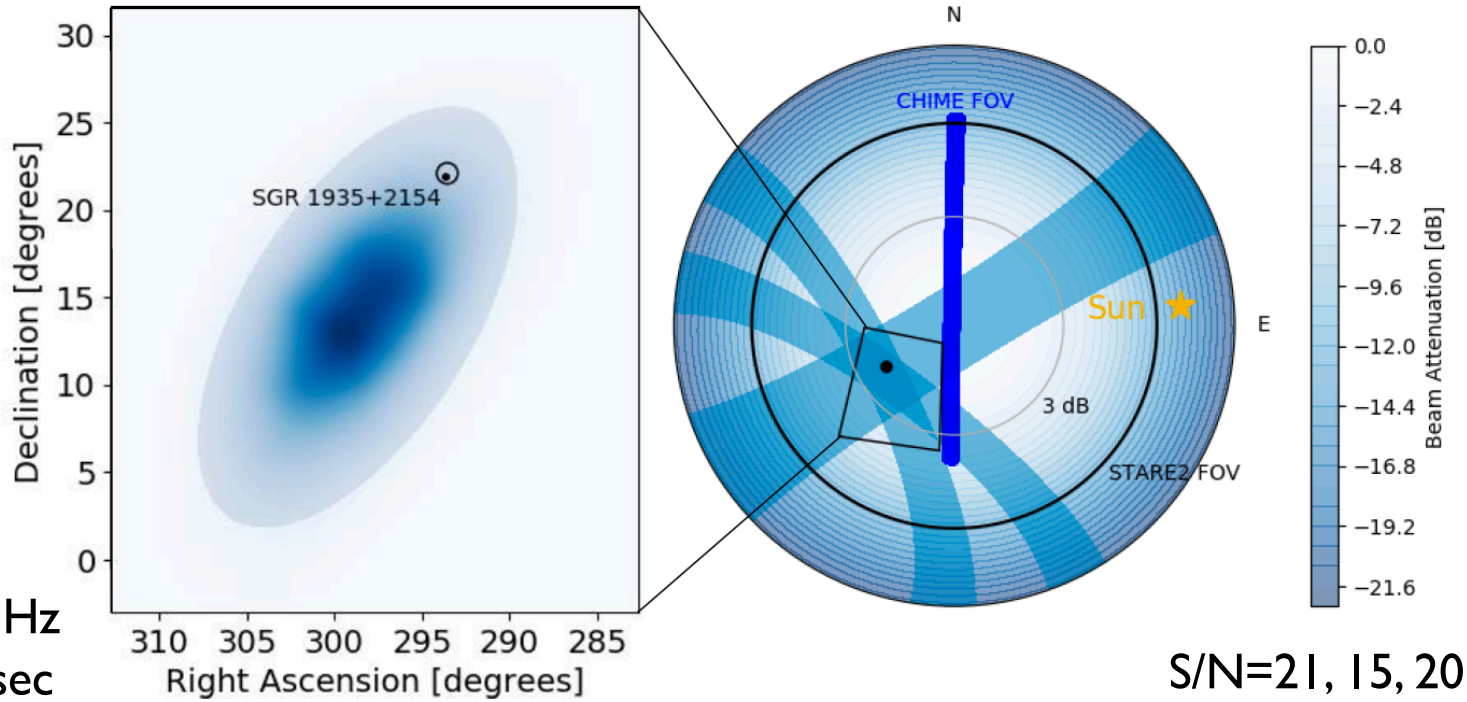

1281-1468 MHz

Δt=65.536 μsec

Δν=122.07 kHz

S/N=21, 15, 20

Figure 2: **STARE2 localisation of ST 200428A.** *Right:* An altitude and azimuth view of the sky at the OVRO STARE2 station at the time ST 200428A was detected. The large black circle corresponds to the STARE2 field of view (FOV), which is set by the edge of a horizon shield at OVRO[3]. A grey circle labelled "3 dB" indicates the zenith angle corresponding to the FWHM of the STARE2 response on the sky. The thick blue line represents the CHIME FOV. The yellow star represents the Sun, which is a common source of STARE2 triggers[3]. The black dot represents the known position of SGR 1935+2154. The three light blue arcs correspond to the 95%-confidence localisations for each individual STARE2 baseline. The black quadrilateral represents the outline of the region shown in the left panel. *Left:* The 95% confidence STARE2 localisation region of ST 200428A is shown as a blue ellipse. The blue gradient corresponds to the probability the burst occurred at that location. The CHIME localisation region[16] corresponds approximately to the black circle. The known position of SGR 1935+2154, which is identical to the position of the weak burst detected by FAST[17], is shown as a black dot.

Bochenek+ 2005.10828

SGR 1935+2154

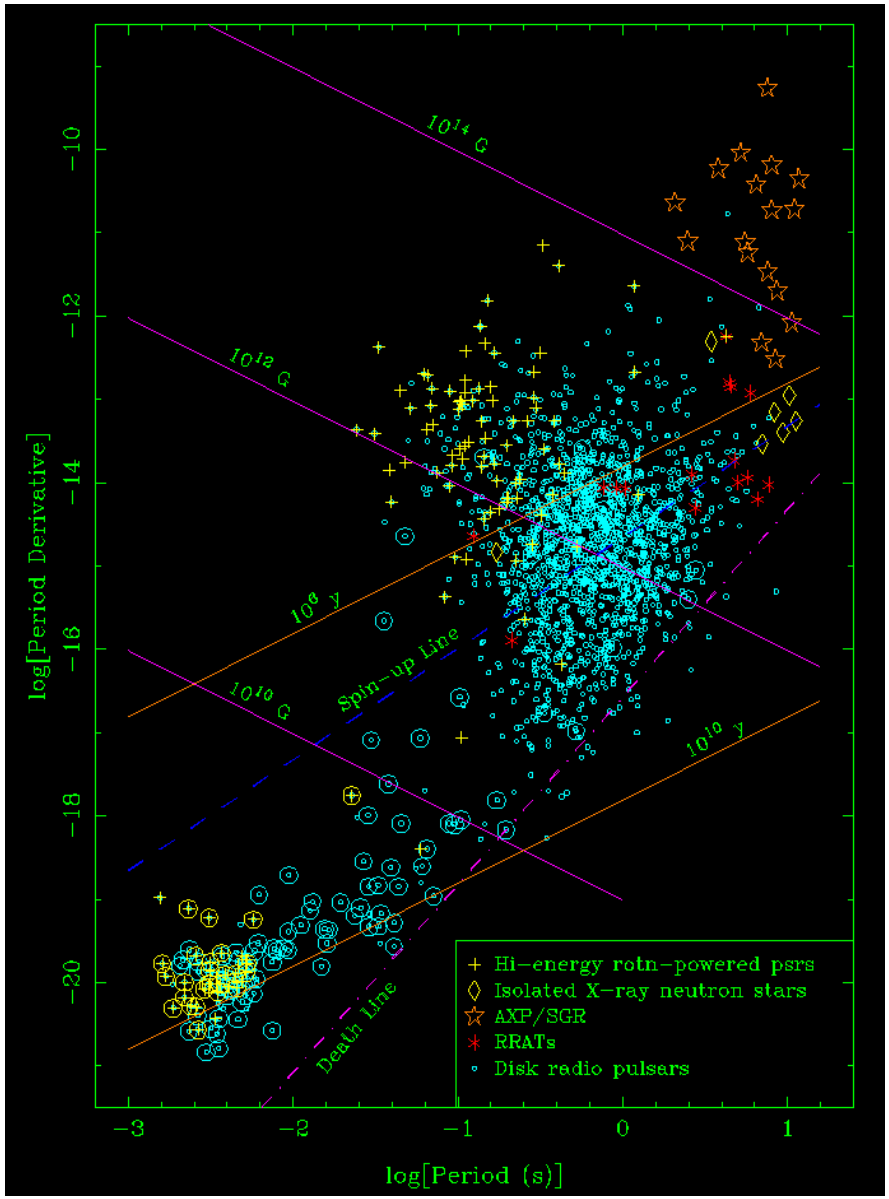

P=3.24 s

Pdot=1.43e-11 s/s

B=2.2e14 G $B^2 \propto P\dot{P}$

d=6.6-12.5 kpc

100 pc above the disk

9 kpc from the GC

at the center of

SNR G57.2+0.8

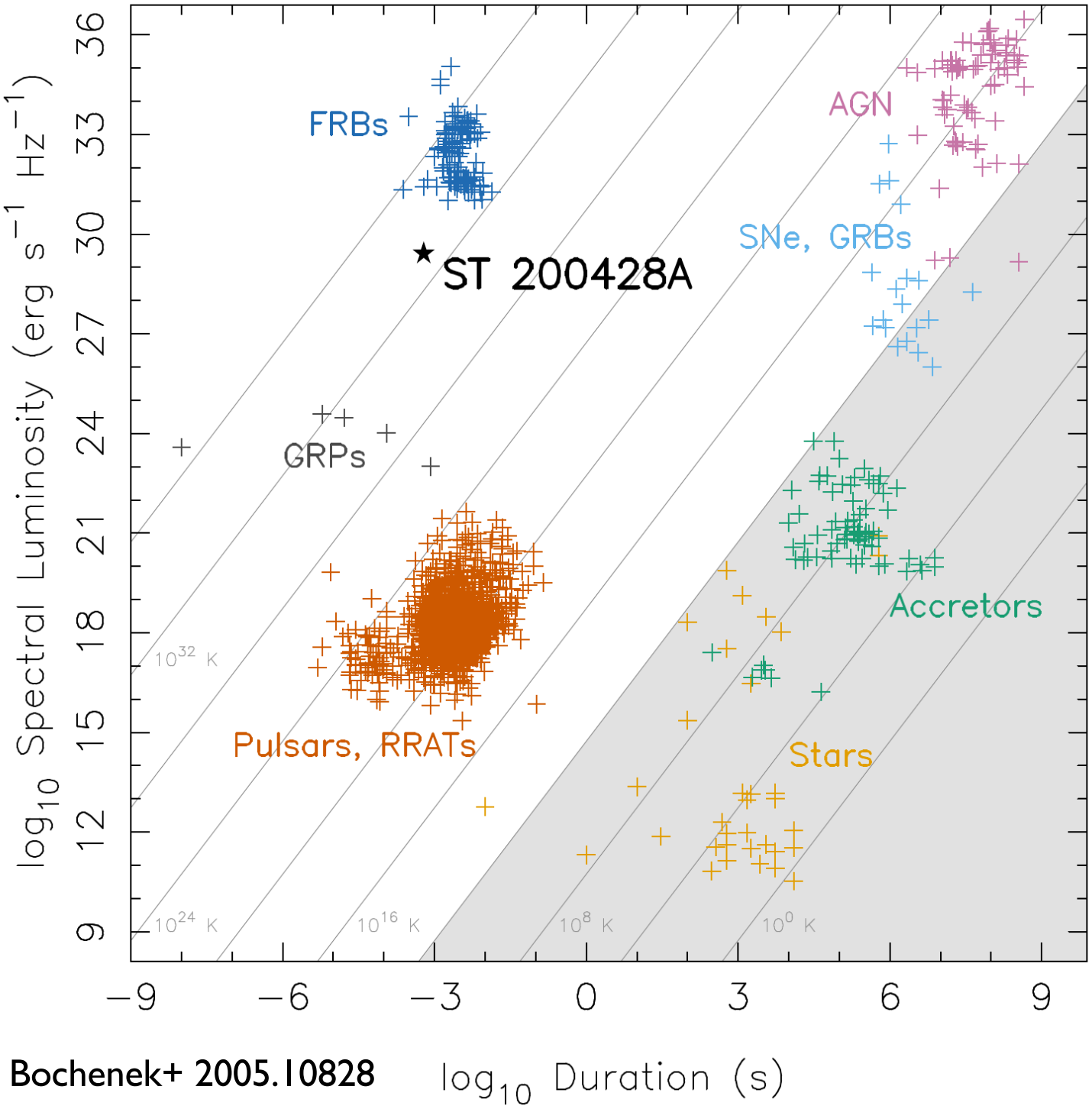

Bochenek+ 2005.10828

Assuming
d=6.5-12.5 kpc

Only FRBs detected at 1-2GHz with known distance

RRAT: rotating radio transients

GRP: max ~ 3e4 Jy ms
~6e31 erg @430MHz

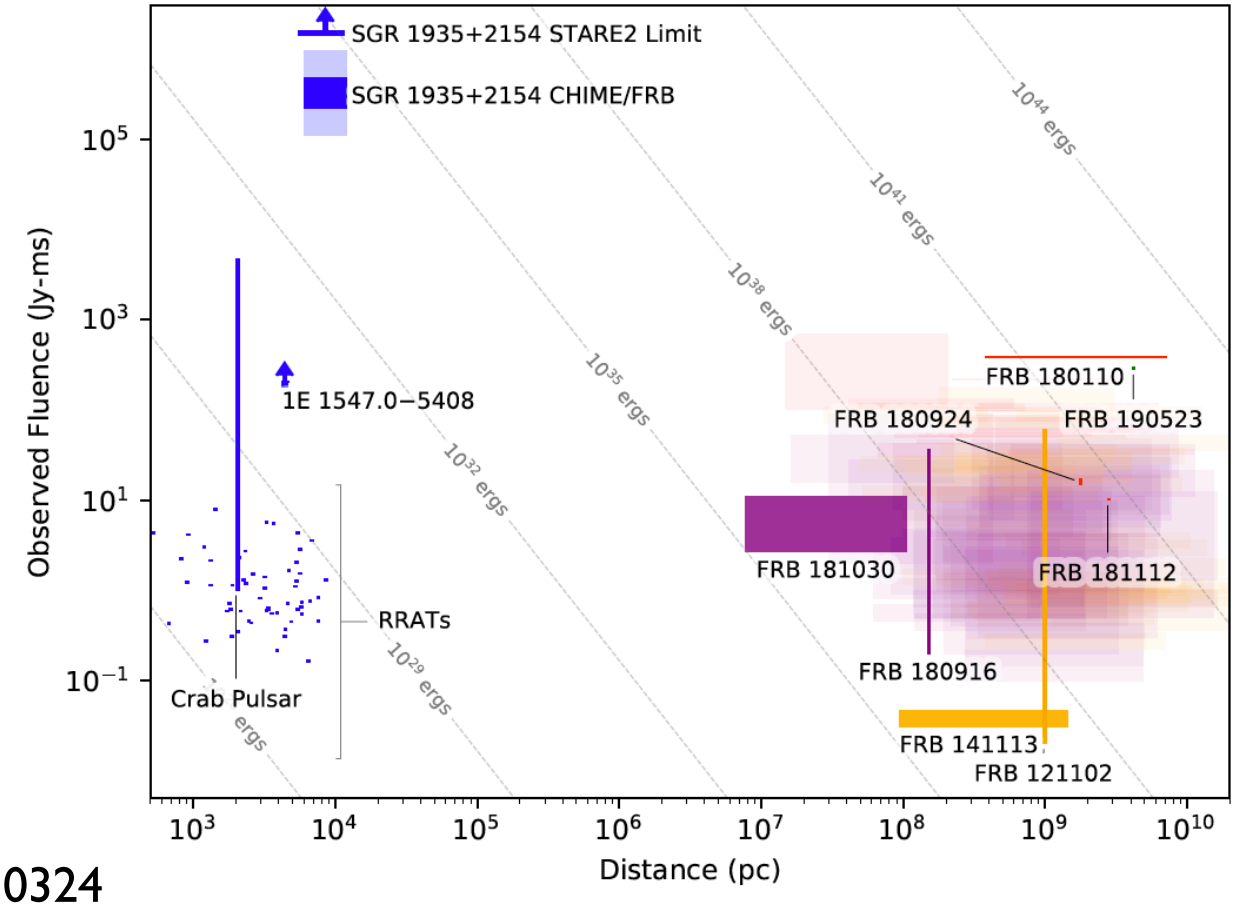

CHIME+ 2005.10324

Figure 2: **Comparison of short radio burst energetics.** The observed burst fluences at radio frequencies from 300 MHz to 1.5 GHz for Galactic neutron stars and extragalactic FRBs are plotted with their estimated distances. The fluence ranges include the uncertainties in fluence measurements as well as ranges of individual bursts for repeating FRBs and pulsars. FRBs colours indicate their detection telescope: CHIME/FRB (purple), ASKAP (red), DSA-10 (green, FRB 190523), Arecibo and Parkes (orange). Galactic sources are plotted in blue. For SGR 1935+2154 the blue rectangle indicates the nominal range of 400–800-MHz fluences measured for the two bursts while the light blue region incorporates the possible systematic uncertainty in the CHIME/FRB fluence as described in the text. The STARE2 lower limit on the fluence at 1.4 GHz is also shown. Gray diagonal lines indicate loci of equal isotropic burst energy with an assumed fiducial bandwidth of 500 MHz. FRB distances are estimated from their extragalactic dispersion measure contribution including the simulated variance [36]. Pulsar distances are estimated based on the NE2001 Galactic electron distribution model [14]. Objects with accurately measured distances (parallax or host galaxy redshift) are indicated with vertical lines.

Galactic FRB from Magnetar Bursts

A smoking gun! But new puzzles arise

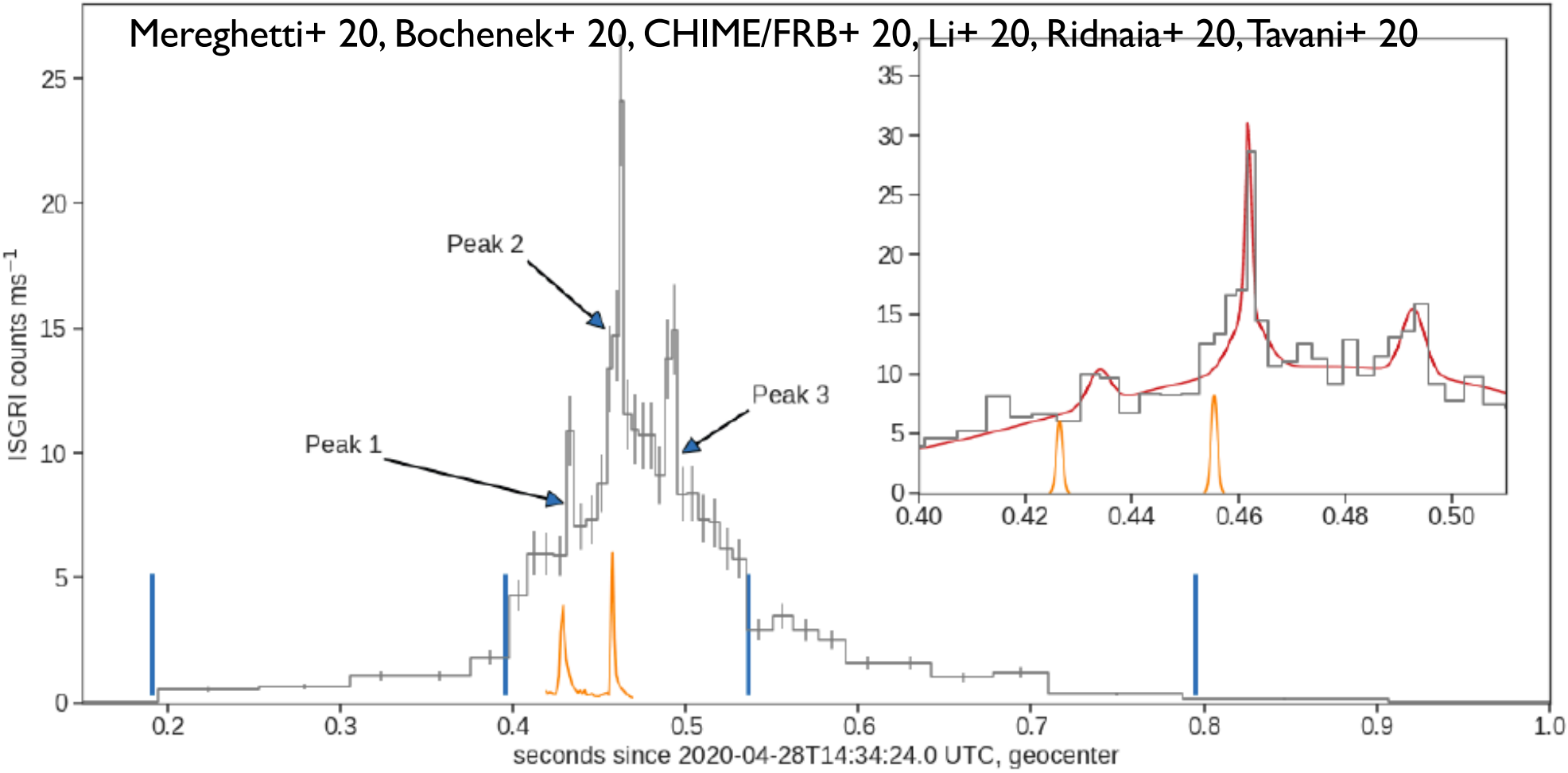

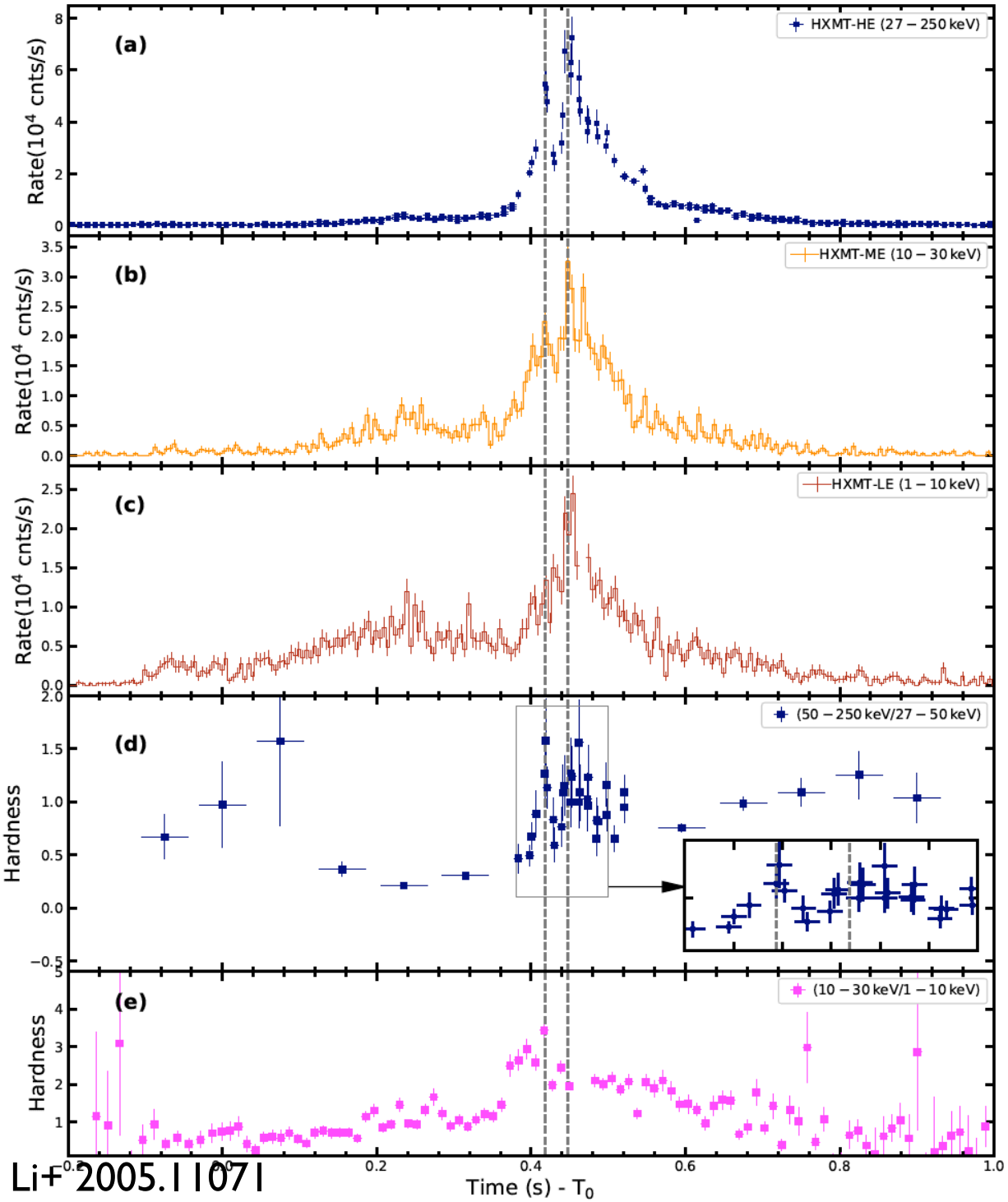

Li+ 2005.11071

Insight-HXMT
$7.14^{+0.41}_{-0.38}$e-7 erg/cm^2
~1e40 erg

HE: 1 ms resolution
near the peak
10 ms outside
ME & LE: 5 ms bin

Saturation near the peak
for HE & LE
Deadtime in ME

T0=14:34:24.0114UT
(geocentric time)

Konus-*WIND*

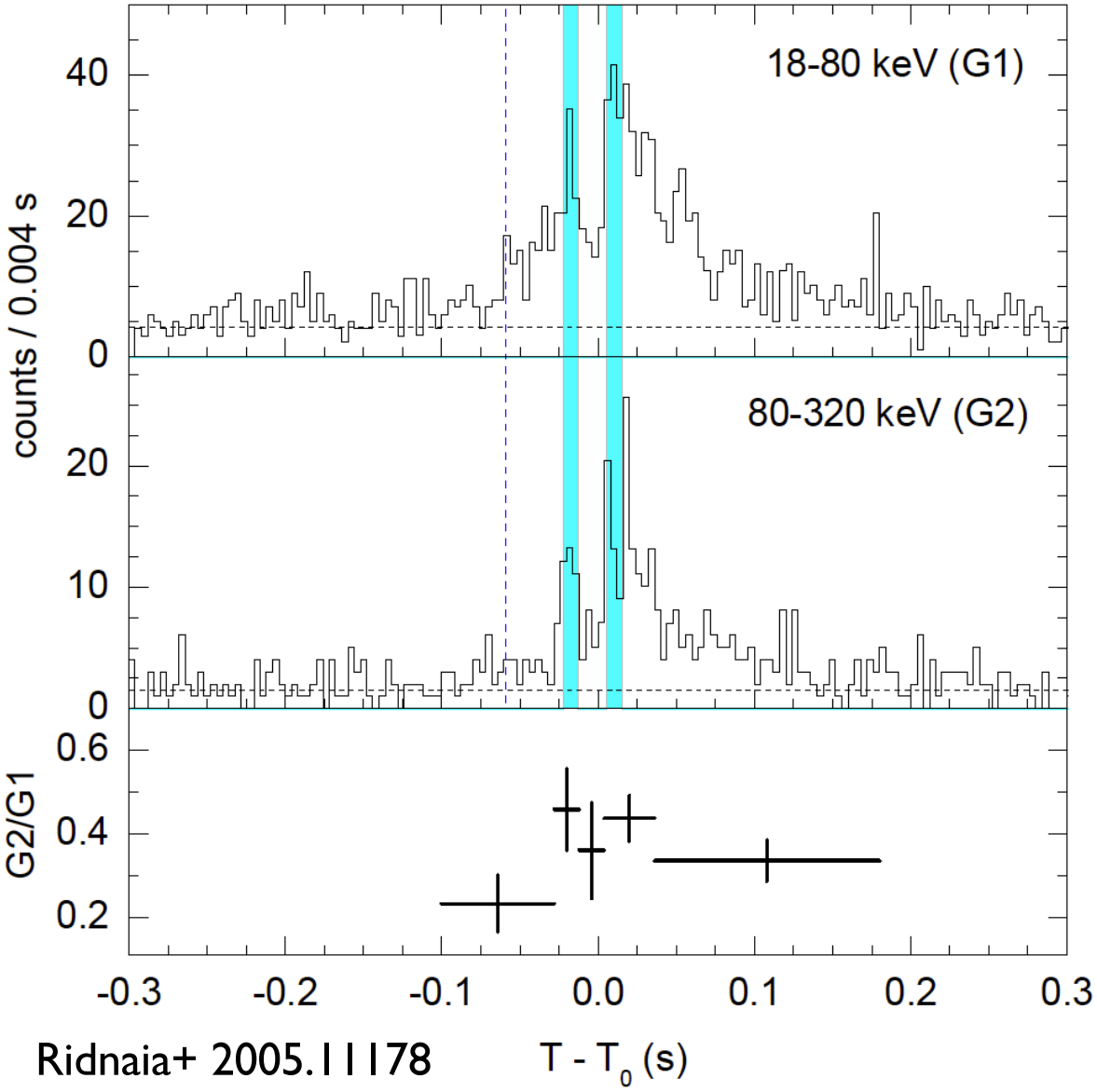

Ridnaia+ 2005.11178

T_0=14:34:24.447 UT
(geocentric time)

AGILE

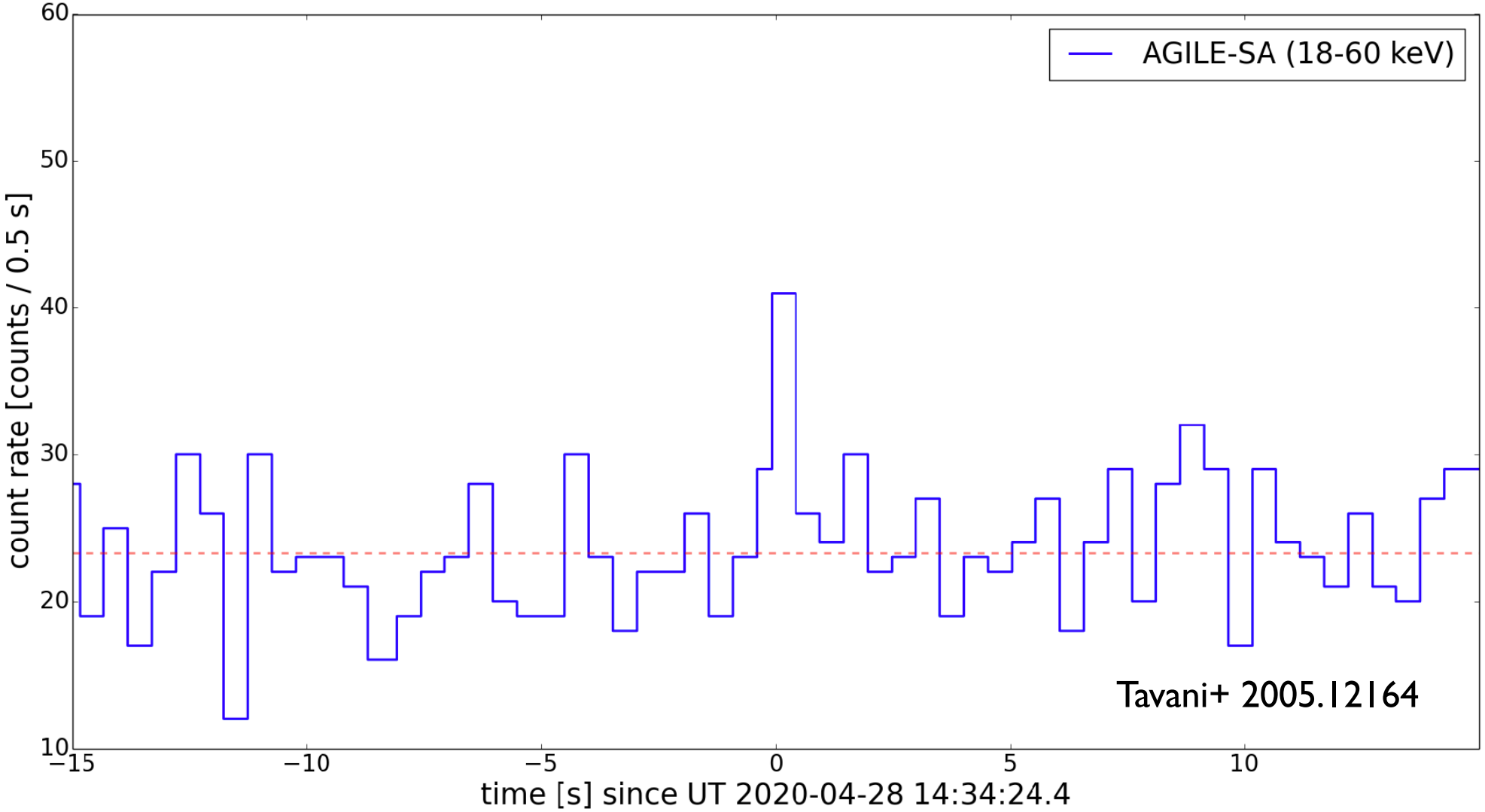

18-60 keV (Super-AGILE), ~0.5 sec, cutoff ~80 keV (No AC signal), ~8.1e39 erg @12 kpc at 121 deg off-axis angle, S/N=3.8σ, post-trial 2.9σ

FRB from a Magnetar!

- Fast radio burst 200428
  - STARE2, CHIME
  - ~MJy, ~msec, E_{radio}~10^{35} erg
- Magnetar SGR 1935+2154 in our Galaxy
- With X-ray bursts
  - E_X~10^{40} erg, E_p~80 keV, E_X/E_{radio}~10^5
  - Other FRBs are >10^8 times fainter
- Cosmological FRBs are also magnetar bursts?

No FRB from Others!?

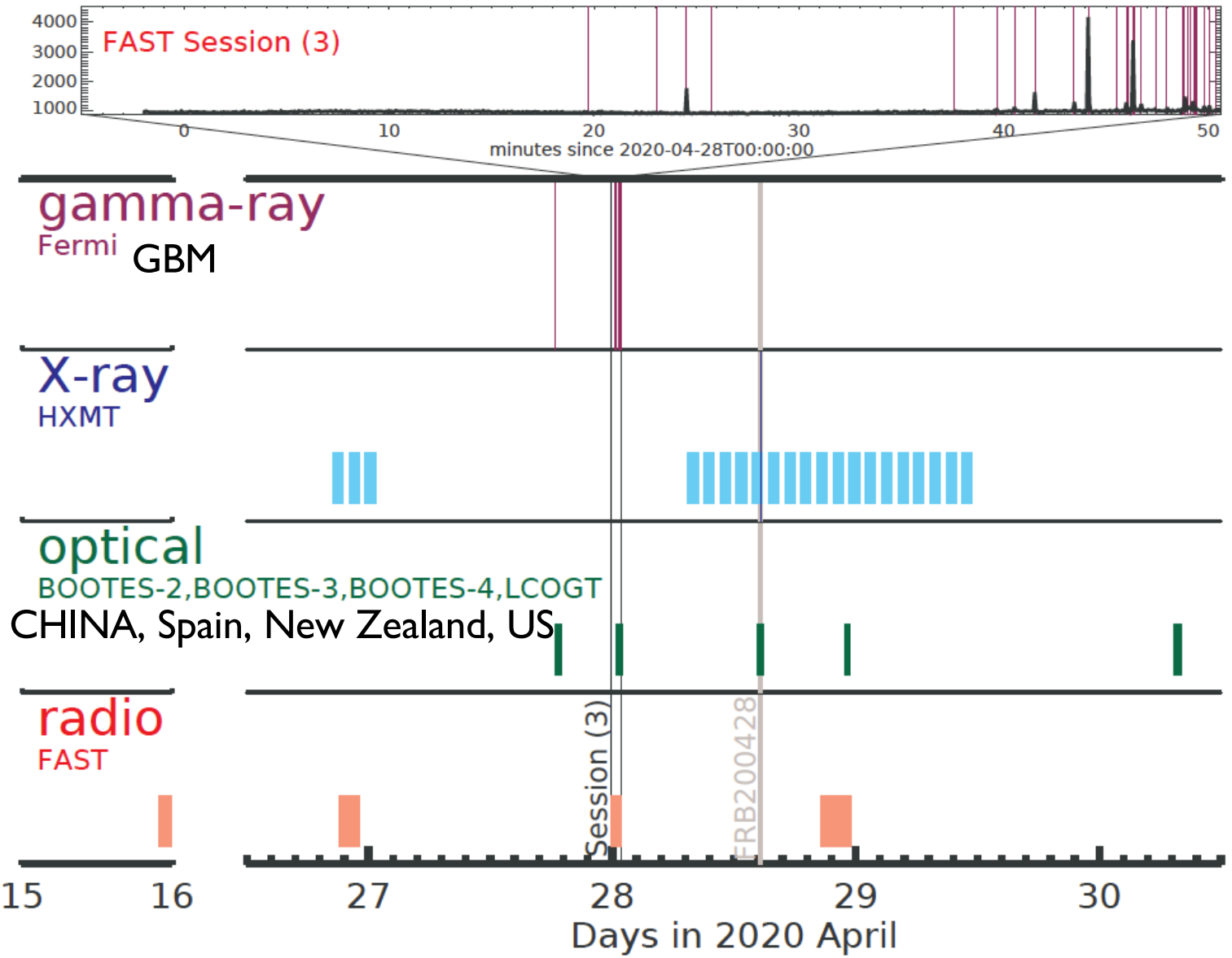

1.25 GHz
460 MHz band

29 bursts
in ~30 min

No radio
to 10-40 mJy ms

8 orders-of-mag
deeper limits

FAST+ 2005.11479

High Temperature!?

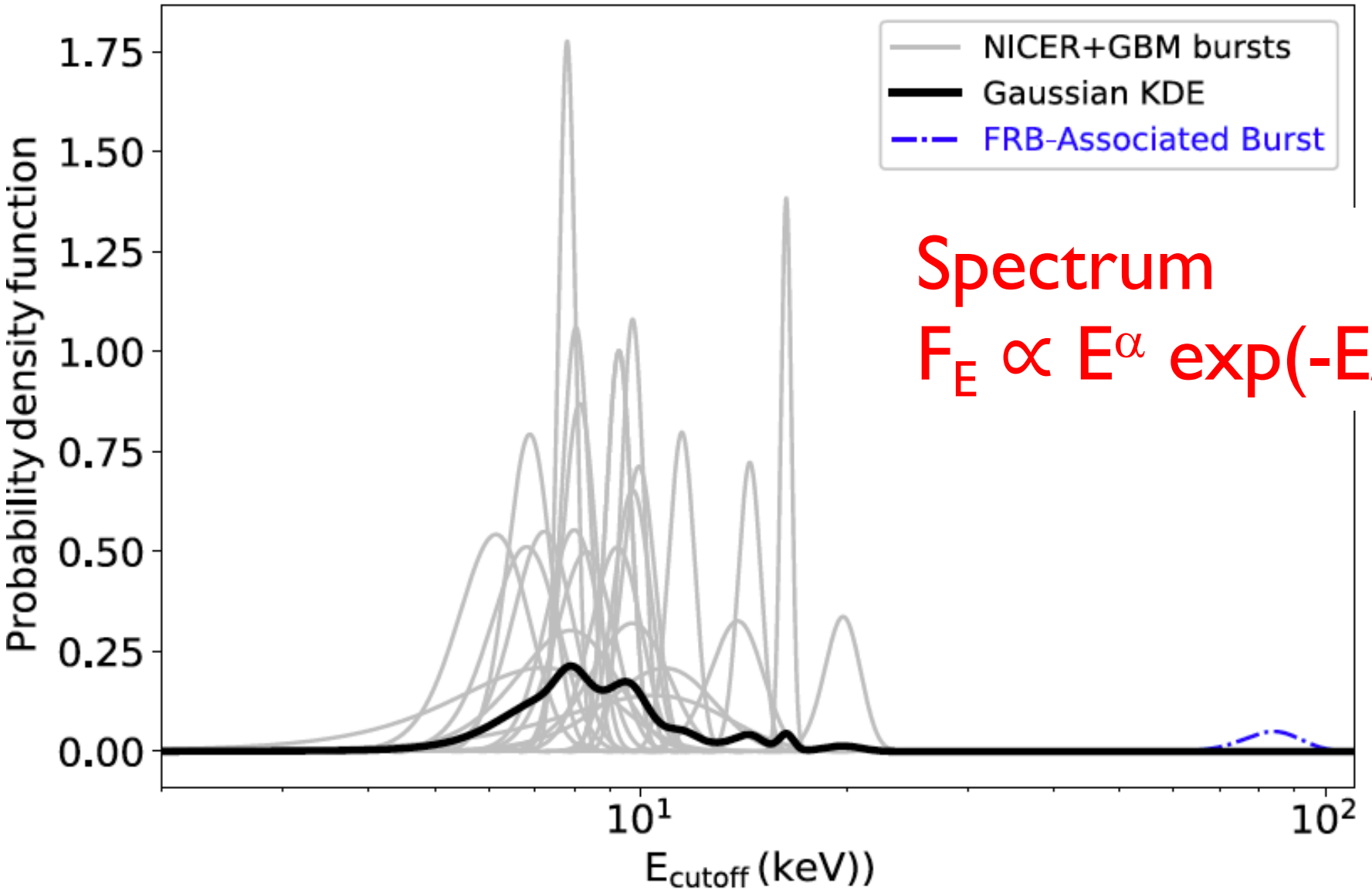

Spectrum

$F_E \propto E^{\alpha} \exp(-E/E_{cut})$

Weaker FRBs w/o X-ray

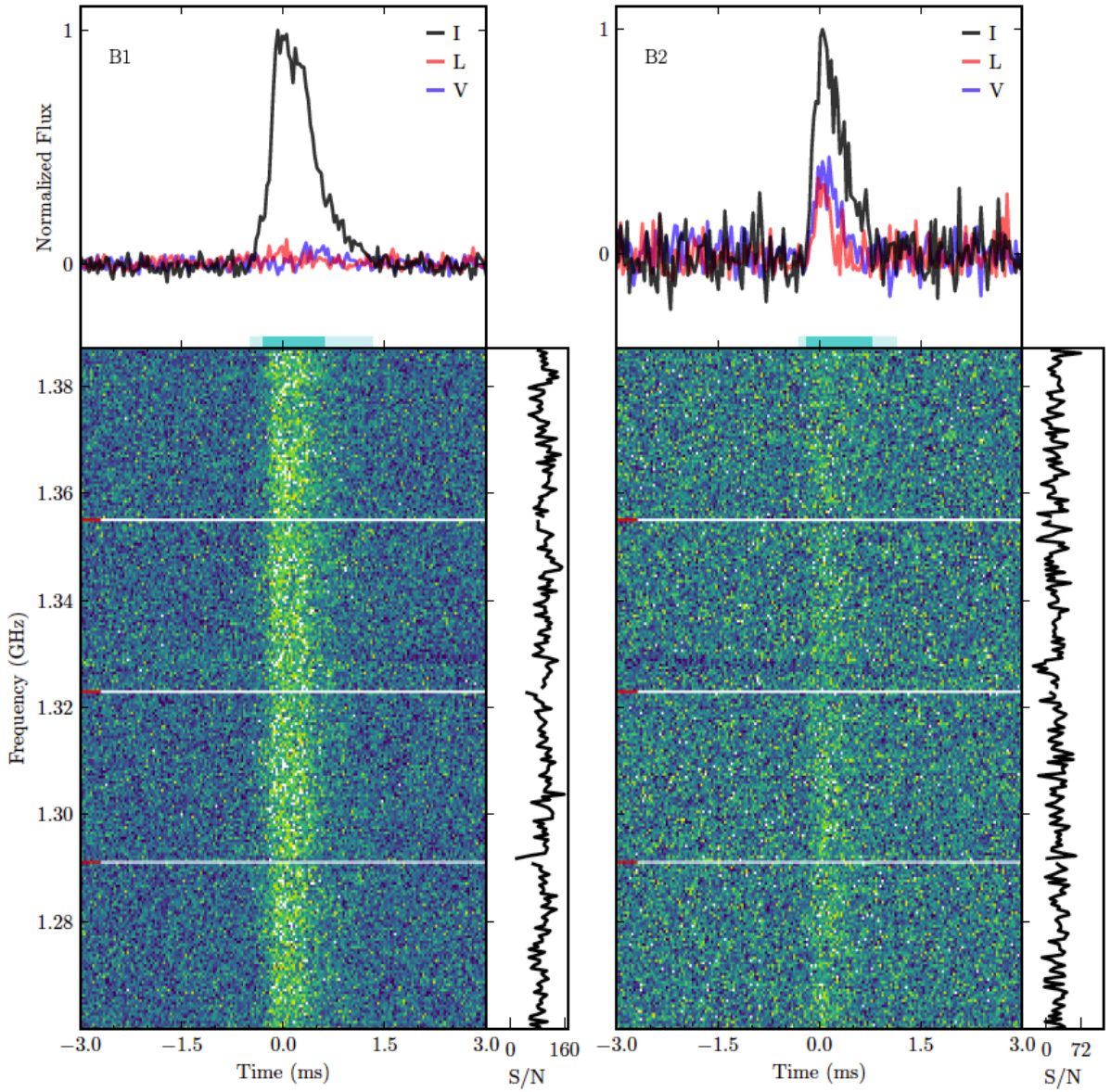

~10^4x fainter bursts

112±22 Jy ms

24±5 Jy ms

separated by 1.4 sec

(43% of P=3.25 sec)

X-ray non-detected

Kirsten+ 20

Galactic FRB from Magnetar Bursts

A smoking gun! But new puzzles arise

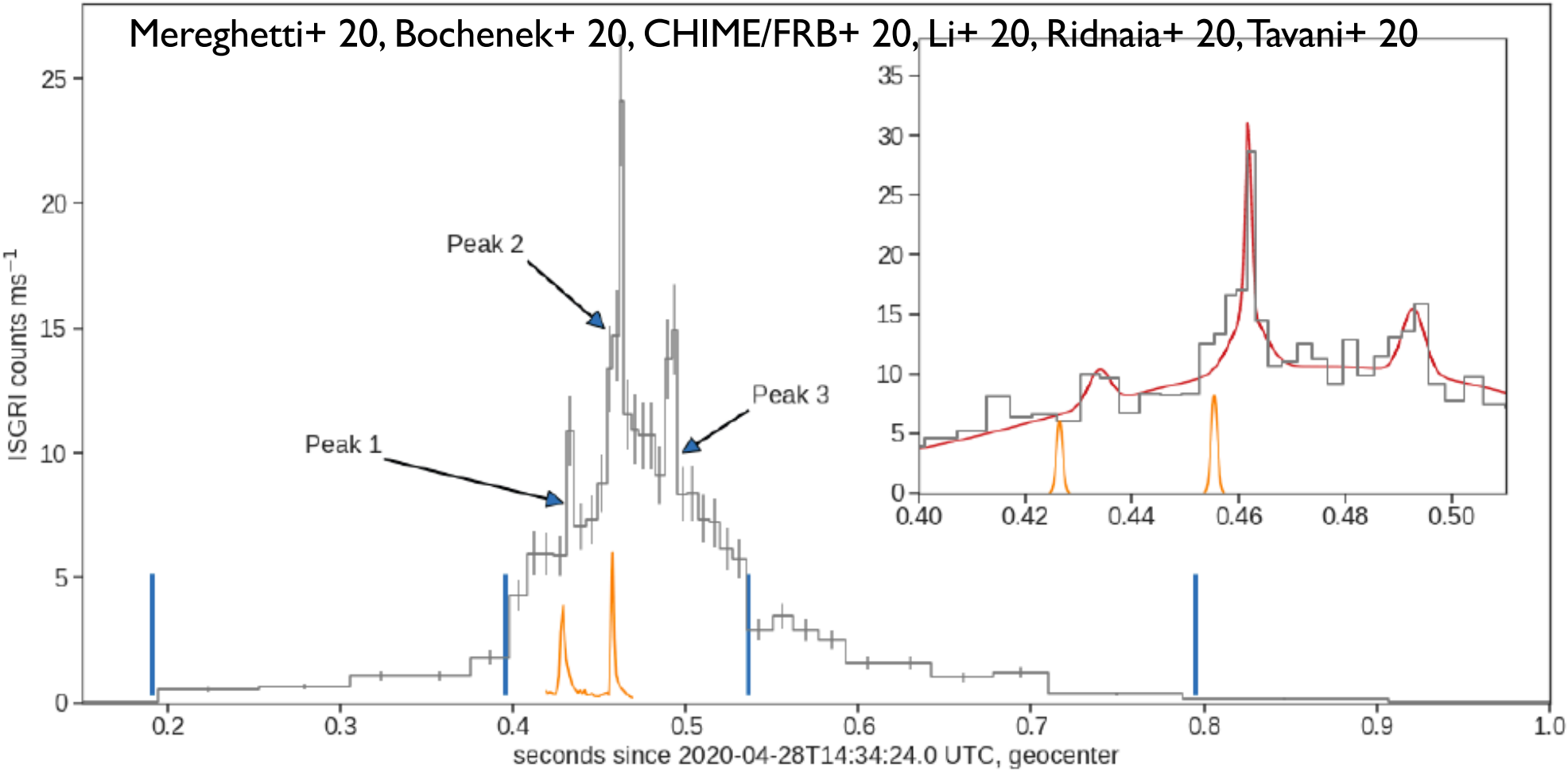

FRB from a Fireball?

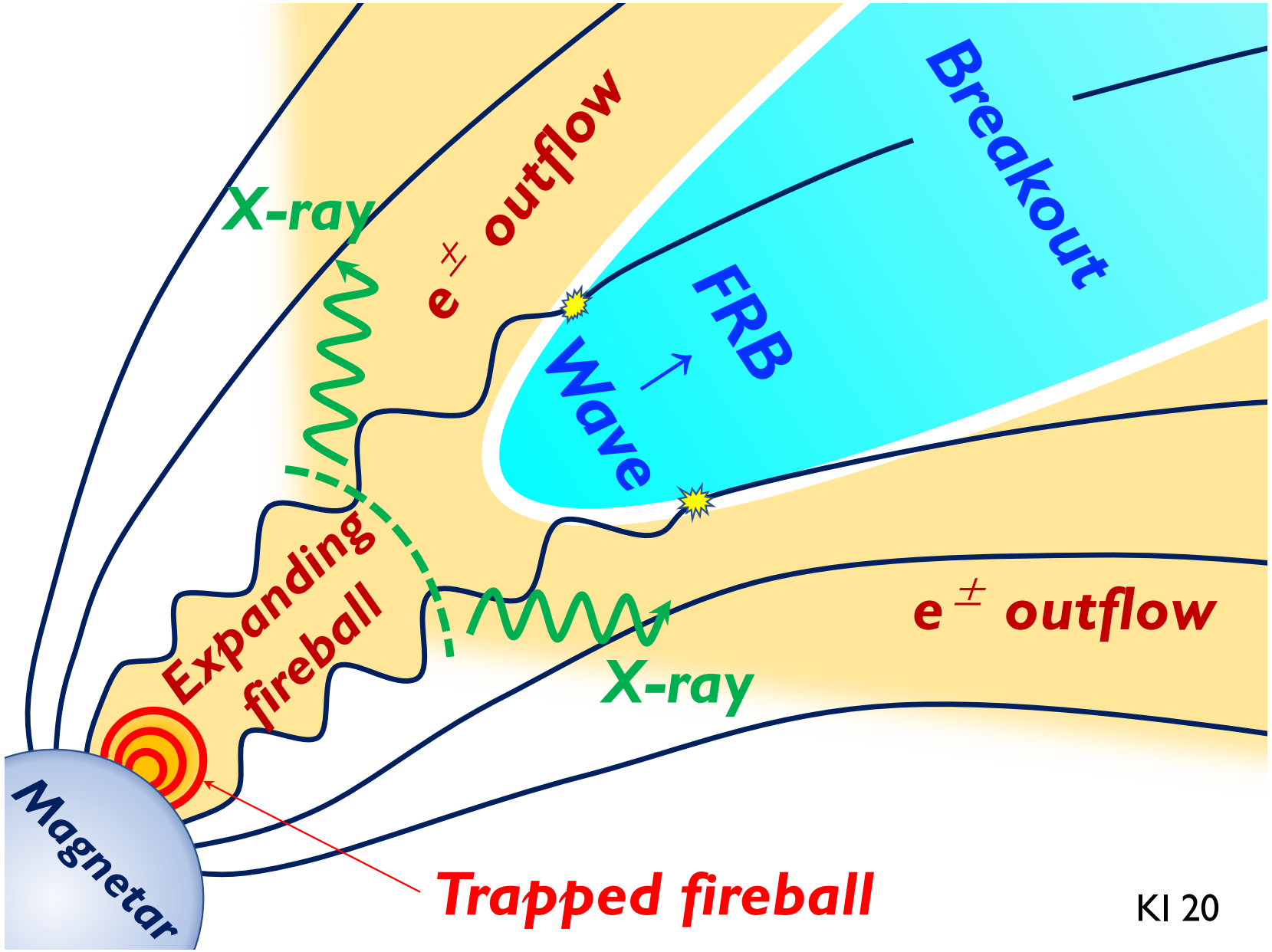

KI 20

Trapped Fireball

Thompson & Duncan 95

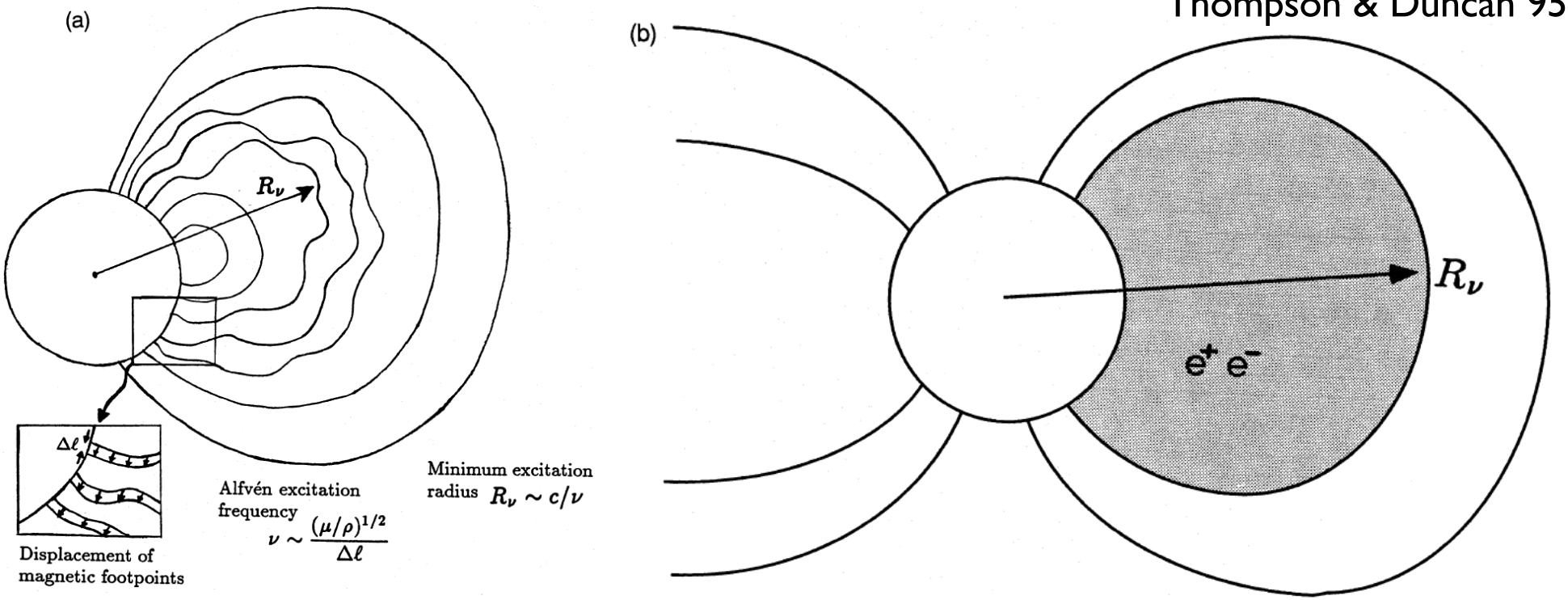

$$\ell_X \sim \left(\frac{L_X}{2\pi c a T^4}\right)^{1/2} \sim 1\times 10^4\,\mathrm{cm}\, L_{X,41}^{1/2} T_{1.9}^{-2},$$

$e^{\pm}$ Creation

Equilibrium number density of $e^{\pm}$

$$n_{\pm} = \frac{eBm_e}{(2\pi^3)^{1/2}\hbar^2}\left(\frac{T}{m_e c^2}\right)^{1/2} \exp\left(-\frac{m_e c^2}{T}\right),$$

Optical depth

$$\tau_{\perp} = \frac{4\pi^2}{5}\sigma_T \left(\frac{T}{m_e c^2}\frac{B_Q}{B}\right)^2 n_{\pm}\ell_X,$$

$$B_Q = m_e^2 c^3/\hbar e = 4.4\times 10^{13}\,\mathrm{G}.$$

Optical Depth

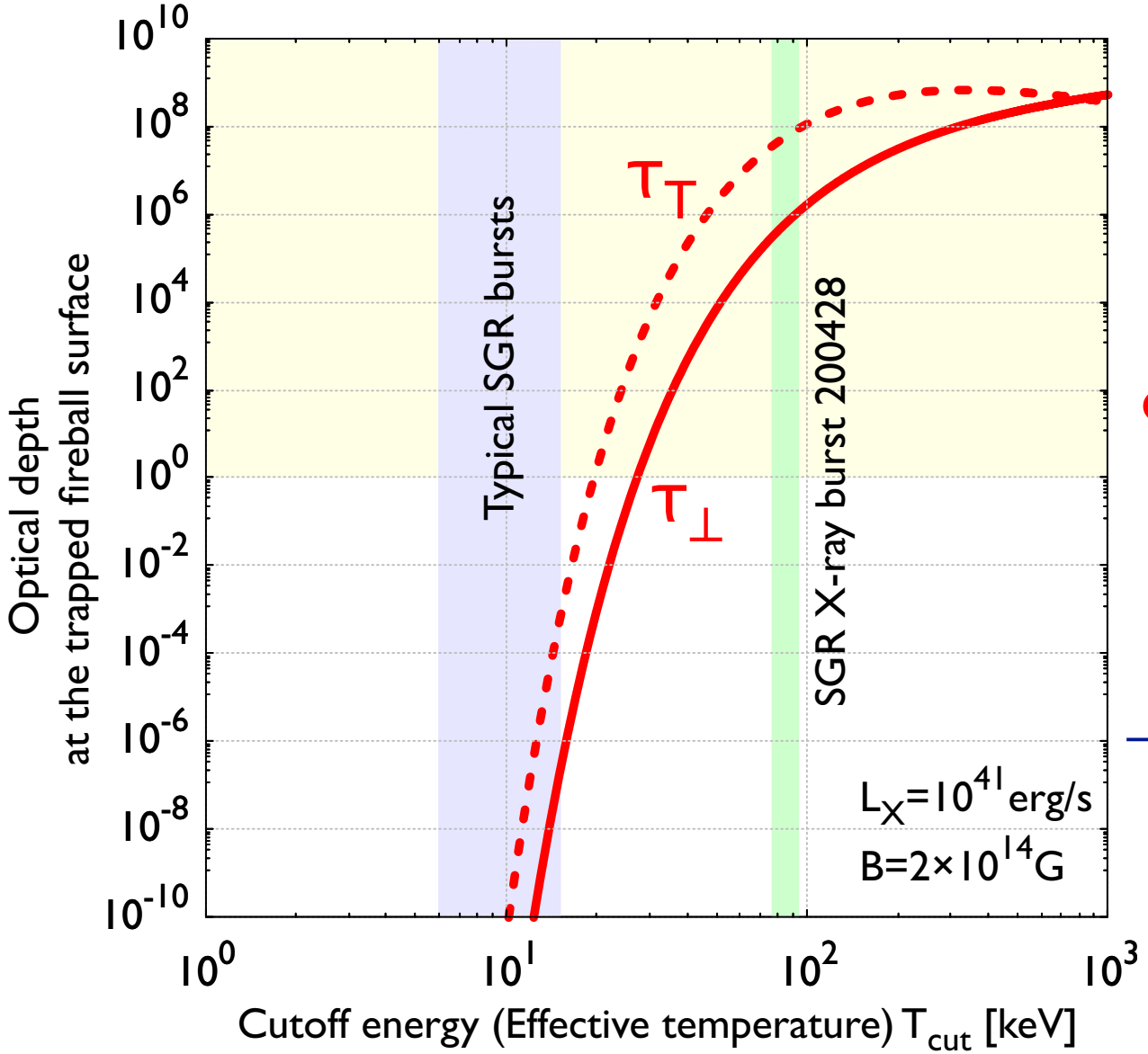

$\tau >> 1$ at the surface of the trapped fireball

X-rays creat $e^{\pm}$
$\rightarrow$ Expanding fireball
$\rightarrow$ $e^{\pm}$ outflow & X-ray

KI 20

Trapped-Expanding FB

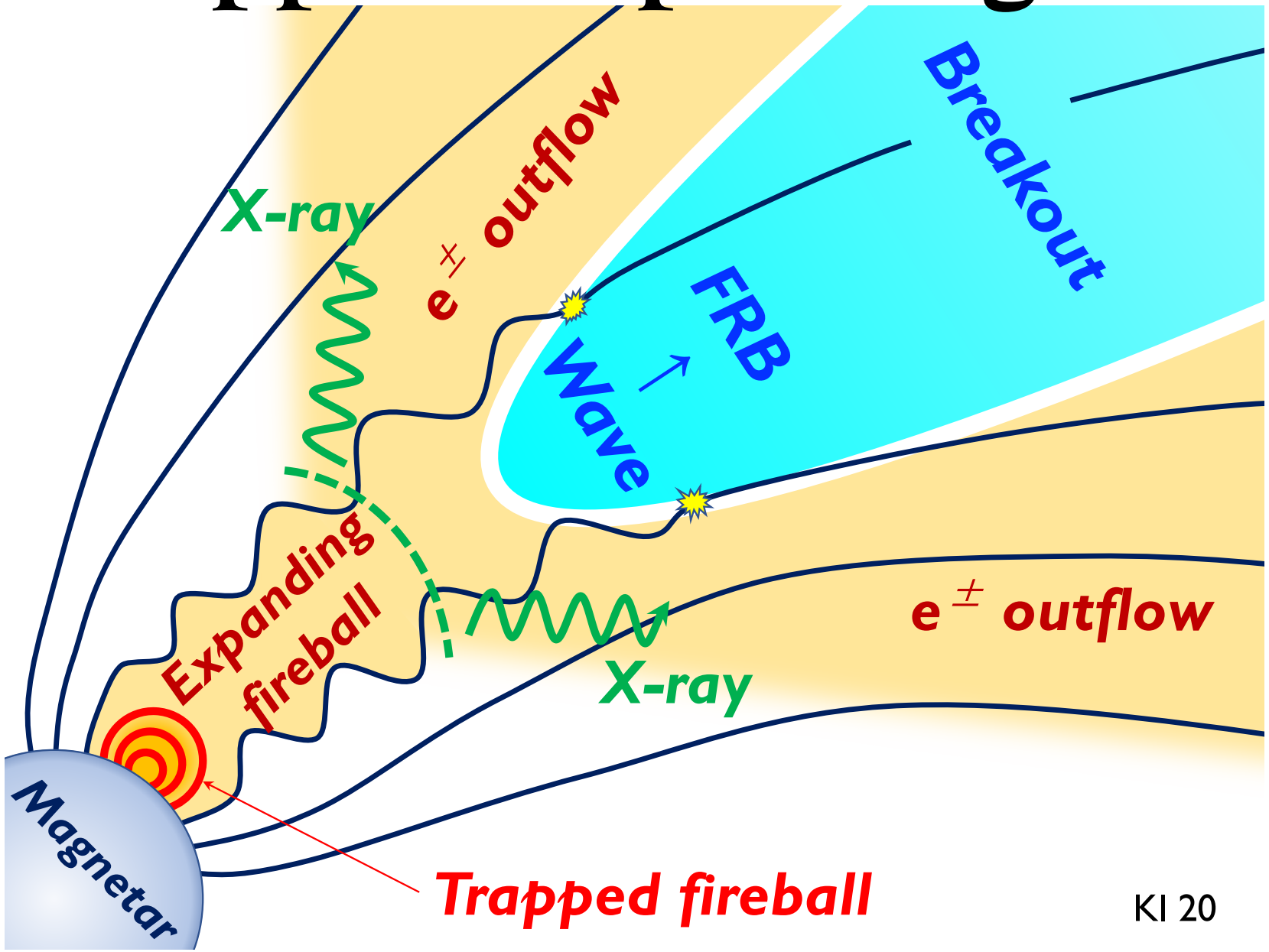

KI 20

$e^{\pm}\gamma$ Diffusion across B

Fireball acceleration

$$\Gamma \sim (r/R)^{3/2}, \quad T' \sim T_{\rm cut}(r/R)^{-3/2}.$$

Diffusion condition

$$t'_{\rm diff} \equiv \frac{\ell_\perp}{c}\tau_\perp < \frac{r}{c\Gamma} \equiv t'_{\rm dyn},$$

is satisfied at

$$r = r_d \sim 1.9R, \quad \Gamma = \Gamma_d \sim 2.6,$$

$e^{\pm}$ Outflow

Annihilation freezes out at $t_{ann} \sim t_{dyn}$

$$n'_{\pm}(r_d) \sim \frac{\Gamma_d}{\sigma_T r_d} \sim \frac{\Gamma_d^{1/3}}{\sigma_T R} \sim 2 \times 10^{18}\,\mathrm{cm}^{-3}\,\Gamma_{d,0.4}^{1/3},$$

$e^{\pm}$ Outflow

$$n'_{\pm}(r) \sim \frac{\Gamma_d^{1/3}}{\sigma_T R}\frac{\Gamma_d}{\Gamma_{\pm}}\left(\frac{r}{r_d}\right)^{-3} \sim 3 \times 10^{16}\,\mathrm{cm}^{-3}\,\Gamma_{d,0.4}^{10/3}\Gamma_{\pm}^{-1} r_7^{-3}$$

$$L_{\pm} \sim 4\pi r^2 n'_{\pm}(r) m_e c^3 \beta_{\pm}^3 \Gamma_{\pm}^2 \sim \frac{4\pi R m_e c^3}{\sigma_T}\beta_{\pm}^3 \Gamma_{\pm}\Gamma_d^{10/3}\left(\frac{r}{R}\right)^{-1}$$

$$\sim 1 \times 10^{36}\,\mathrm{erg\,s^{-1}}\,\beta_{\pm}^3 \Gamma_{\pm}\Gamma_{d,0.4}^{10/3} r_7^{-1}, \qquad (17)$$

$L_X \sim 10^{41}$ erg/s, $L_{FRB} \sim 10^{38}$ erg/s

Compton Drag

Compton drag due to X-rays is very strong

$t'_{\rm dr} = m_e c^2 / c\sigma_T u'_X$ is shorter than

$t'_{\rm dyn} = r/c\Gamma_\pm$

$$u'_X = L_X/4\pi r^2 c\Gamma_\pm^2$$

if $$\Gamma_\pm < \left(\frac{L_X\sigma_T}{4\pi m_e c^3 r}\right)^{1/3} \sim 30\, L_{X,41}^{1/3} r_7^{-1/3}$$

i.e., in the magnetosphere

The velocity of the $e^\pm$ outflow is forced to be

$$\beta_\pm = \cos\theta_{kB},$$

when the photons stream at an angle θ_{kB} with respect to B

Induced Compton

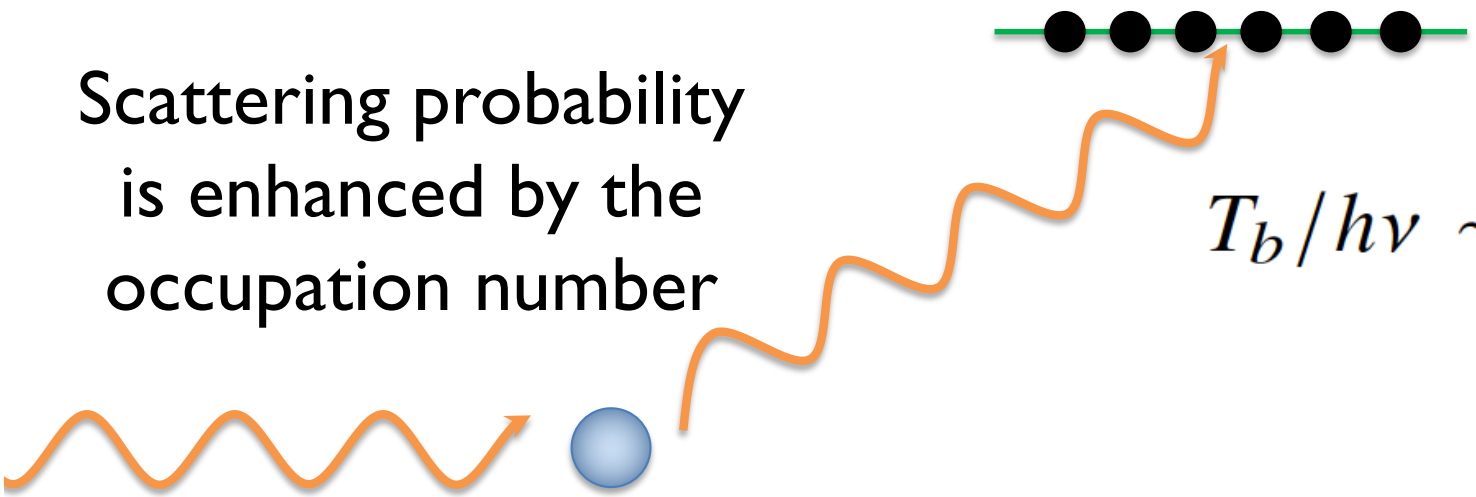

Scattering probability is enhanced by the occupation number

$$T_b/h\nu \sim 10^{34}\, T_{b,33}\nu_9^{-1}$$

Wilson & Rees 78, Thompson+ 94, Lyubarsky 08

$$\tau_T \sim n'_\pm \sigma_T r/\Gamma_\pm \sim 0.2\,\Gamma_{d,0.4}^{10/3}\Gamma_\pm^{-2} r_7^{-2}.$$ **Thomson thin**

$$\tau_C \sim \frac{3\sigma_T}{32\pi^2}\frac{n_\pm(r) L_{\rm FRB} c\Delta t_{\rm FRB}}{r^2 m_e \nu^3}$$

$$\sim 6\times 10^{21}\,\Gamma_{d,0.4}^{10/3}(L_{\rm FRB}\Delta t_{\rm FRB})_{35}\nu_9^{-3} r_7^{-5},$$ **Thick!**

Breakout Criteria

The work done by FRB γ on $e^{\pm}$ is less than the FRB energy

The pushed $e^{\pm}$ is heated up and
the wasted energy per volume is $\sim n'_{\pm} m_e c^2$
But the actual energy is much more
The Compton cooling takes energy $\sim c\sigma_T u'_X t'_{dyn}$
from a heated electron

$$t'_{dyn} = r/c\Gamma_{\pm}$$

$$u'_{\rm FRB} > n'_{\pm} c t'_{dyn} \sigma_T u'_X = \tau_T u'_X$$

$$1 < \frac{L_{\rm FRB}}{\tau_T L_X} = \frac{L_{\rm FRB}}{L_X} \frac{\Gamma_{\pm}^2}{\Gamma_d^{13/3}} \left(\frac{r}{R}\right)^2$$

$$\sim 2 \times 10^{-2} L_{\rm FRB,38.6} L_{X,41}^{-1} \Gamma_{d,0.4}^{-10/3} \Gamma_{\pm}^2 r_7^2,$$

Breakout

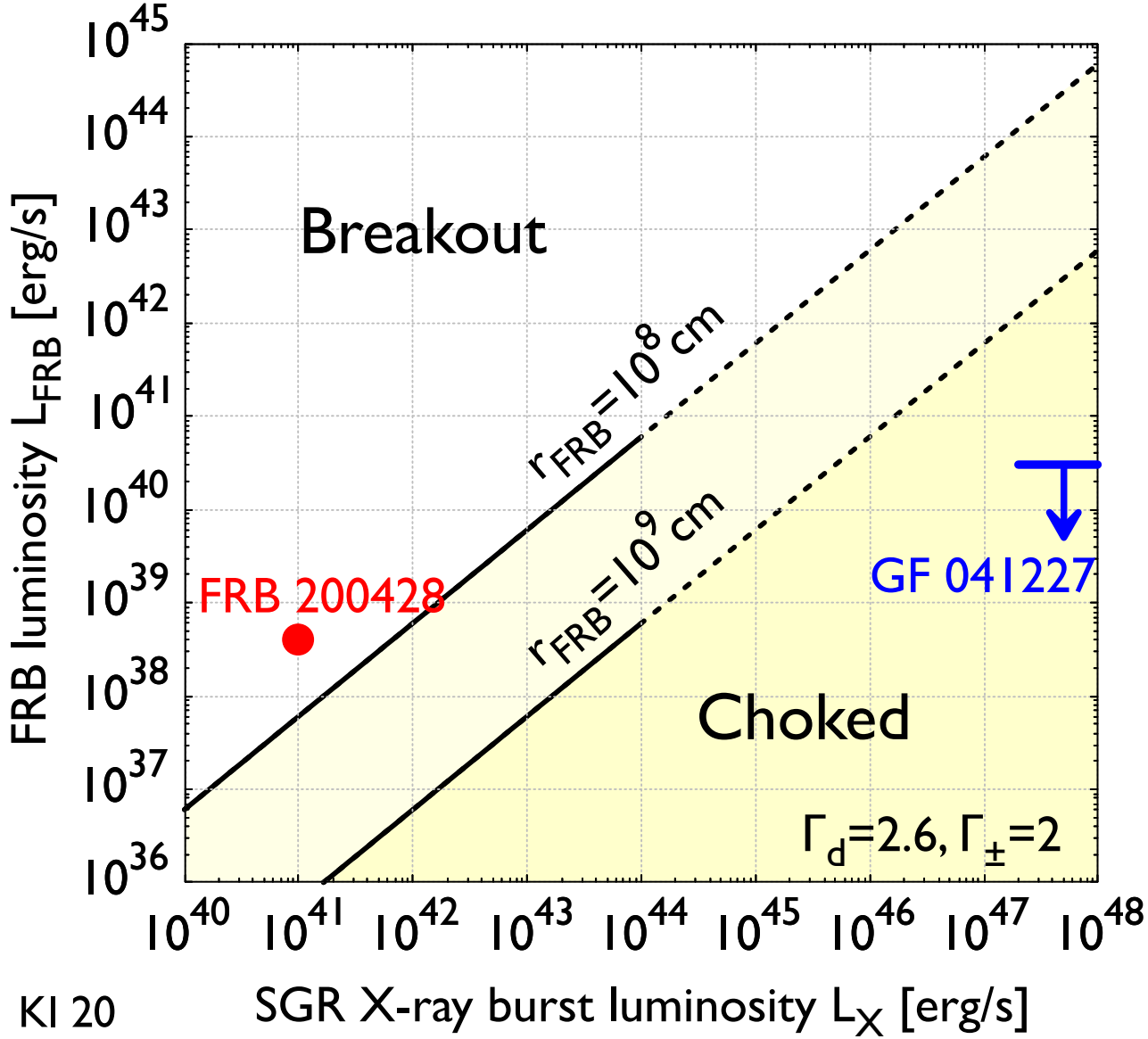

KI 20

$e^{\pm}$ outflow is optically thick to induced Compton

FRB should break out the $e^{\pm}$ outflow

No X-ray burst with weak FRBs

No FRB with bright X-ray bursts

ⓒLi+ @FRB20

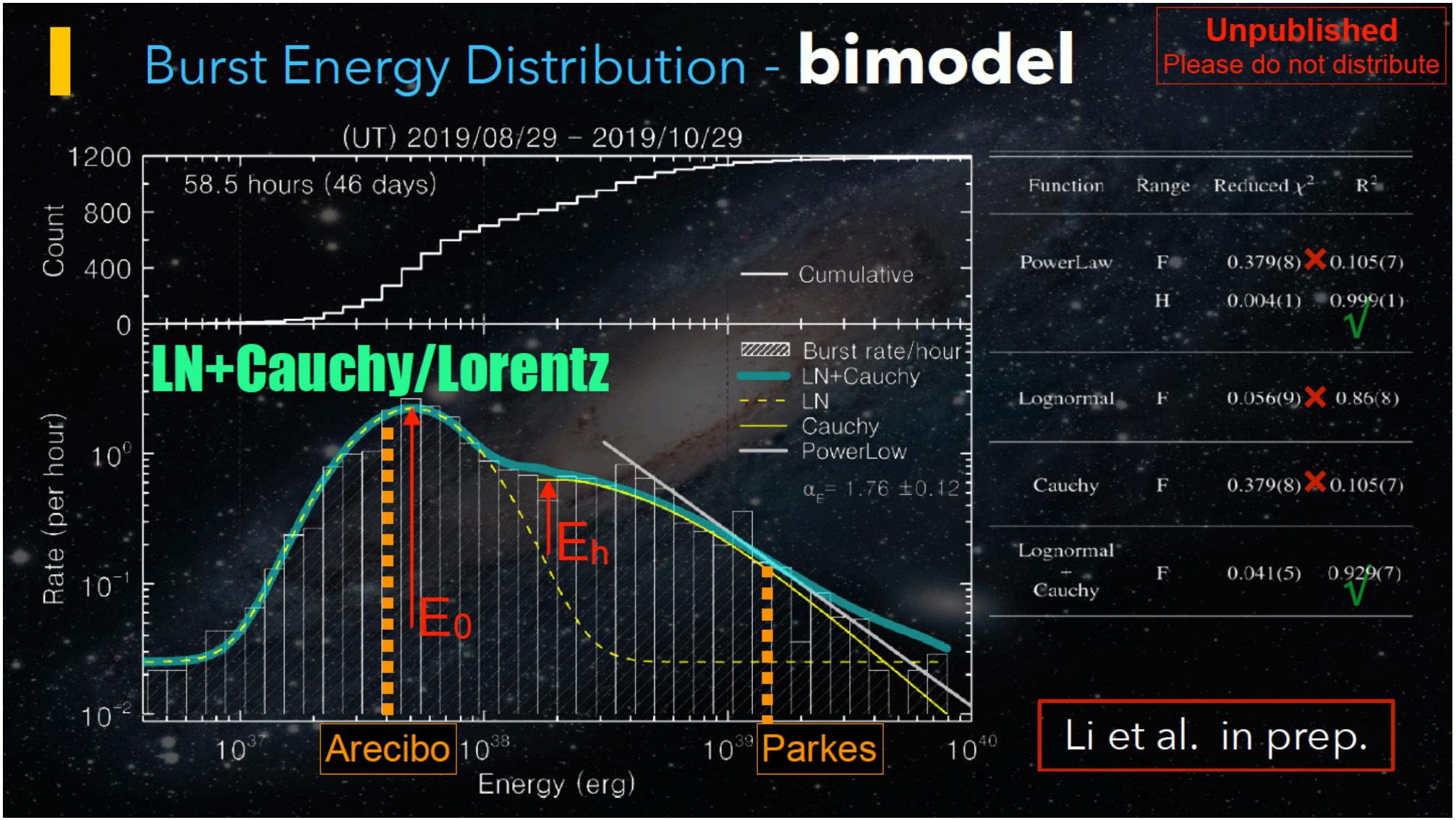

Function	Range	Reduced χ^2	R^2
PowerLaw	F	0.379(8) ✗	0.105(7)
	H	0.004(1)	0.999(1) √
Lognormal	F	0.056(9) ✗	0.86(8)
Cauchy	F	0.379(8) ✗	0.105(7)
Lognormal + Cauchy	F	0.041(5)	0.929(7) √

Future Prospects

GOAL:

Localize Every CHIME-Detected FRB (few thousand) to < 50 mas

4

Interplay w/ Laser Physics

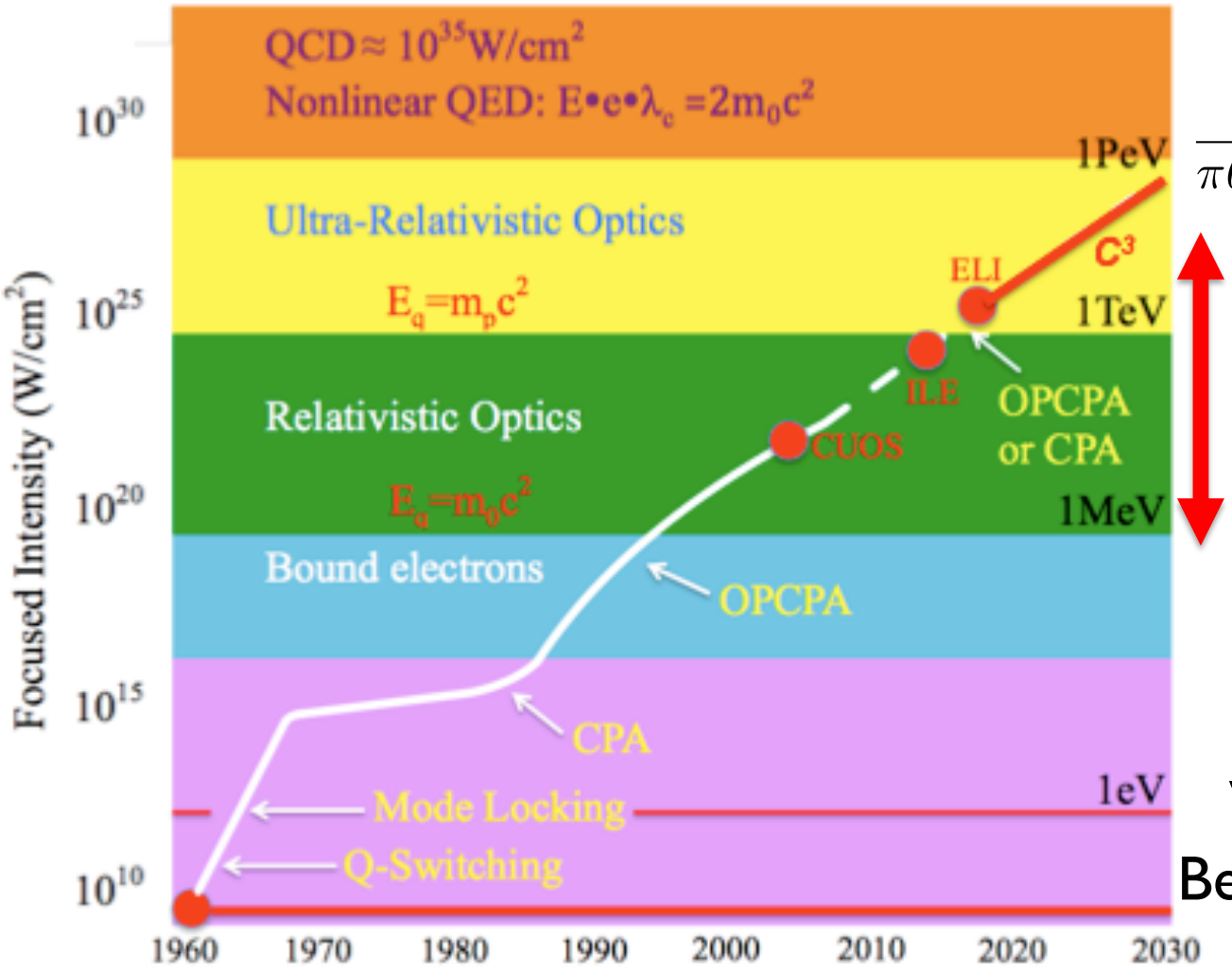

Mourou+ 12

FRB intensity

$$\frac{L}{\pi\theta^2 r^2} \sim 3\times10^{19}\frac{L_{41}}{\theta^2 r_7^2}\,\mathrm{W\,cm^{-2}}$$

$$\sim 3\times10^{27}\frac{L_{43}}{\theta_{-3}^2 r_7^2}\,\mathrm{W\,cm^{-2}}$$

Nonlinear QED
Vacuum polarization
Schwinger effect
Ponderomotive force
Wake field acceleration
Beyond the standard model

Summary

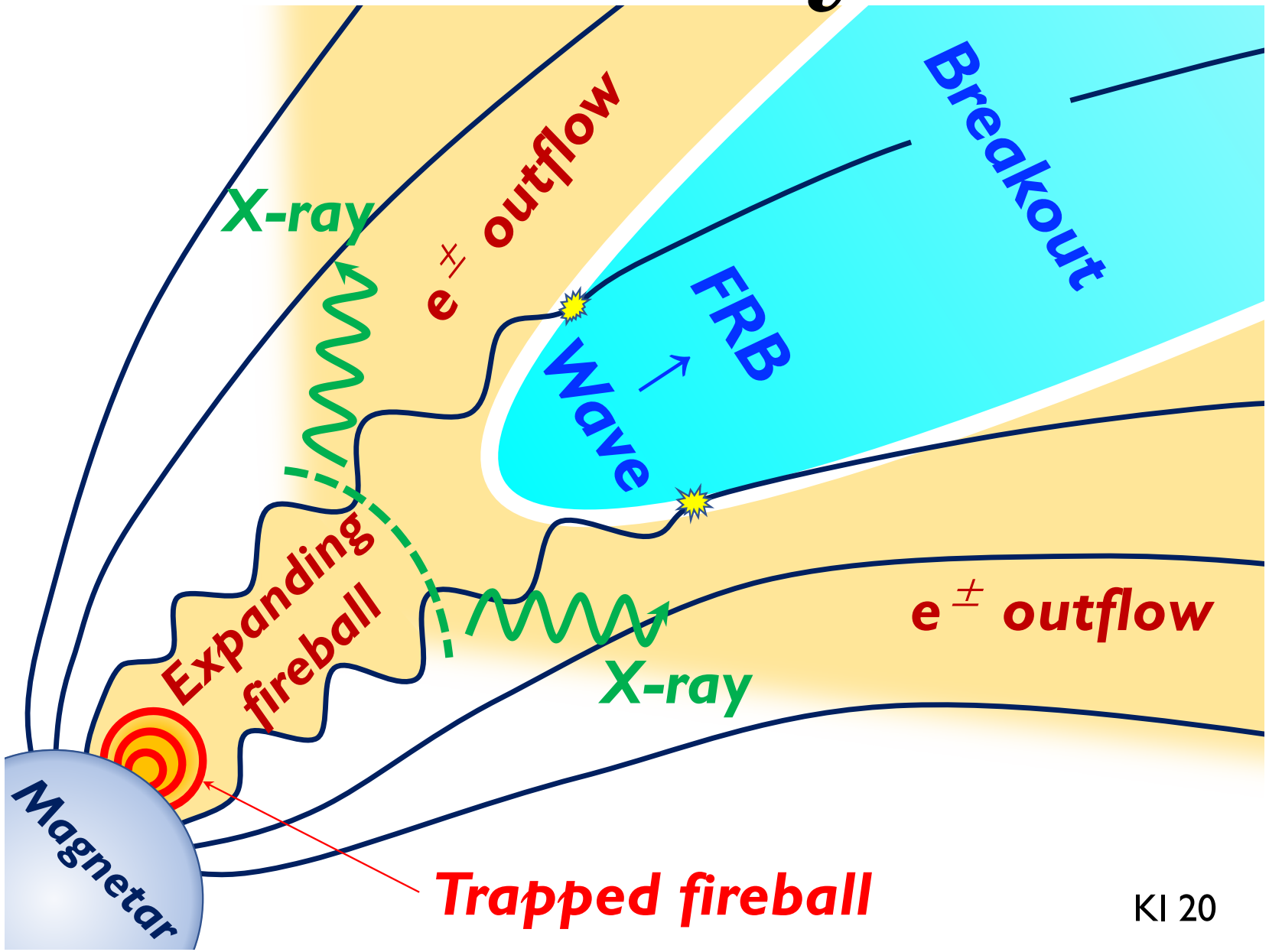

KI 20

Magnetosphere Model

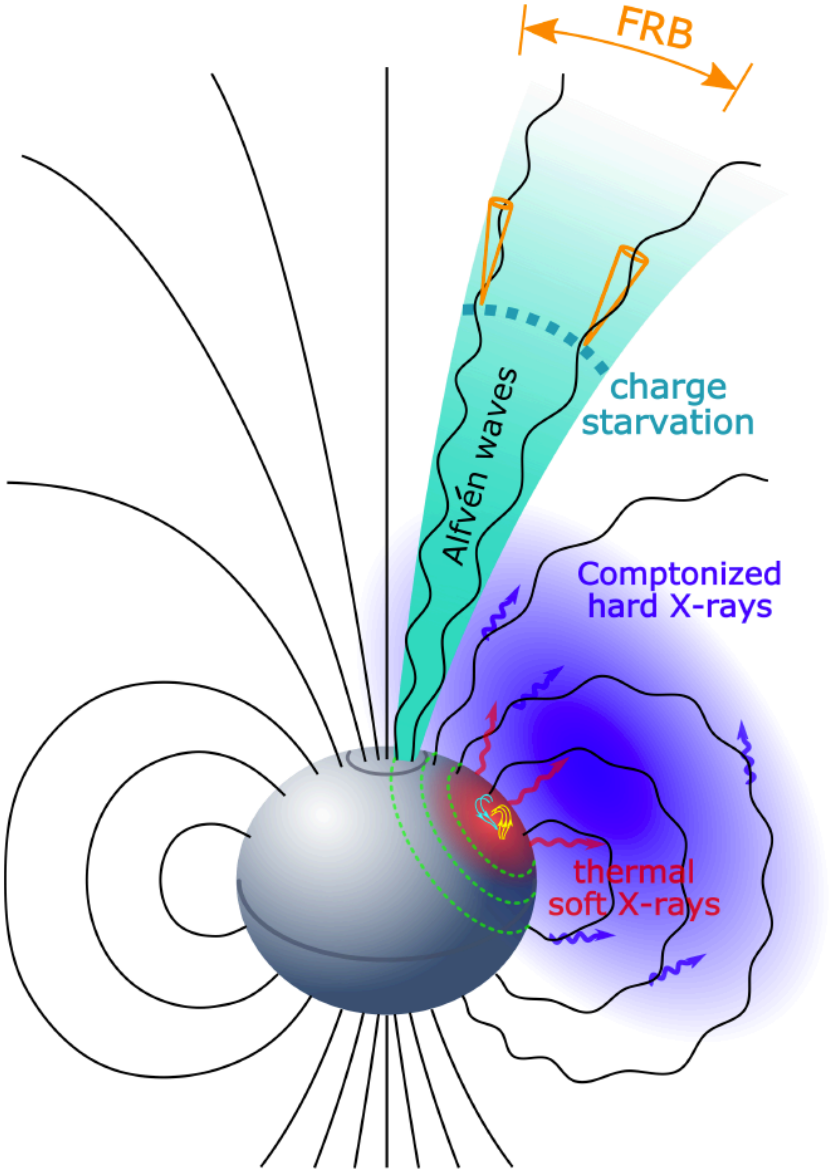

FRB from near-by magentar magnetosphere

Lu et al. 2020; Lyutikov & Popov 2020; Katz 2020; Kashiyama et al. 2013; Cordes & Wasserman 2016; Lyutikov et al. 2016; Kumar et al. 2017; Zhang 2017; Yang & Zhang 2018; Lyubarsky 2020; Kumar & Bošnjak 2020; Ioka & Zhang 2020

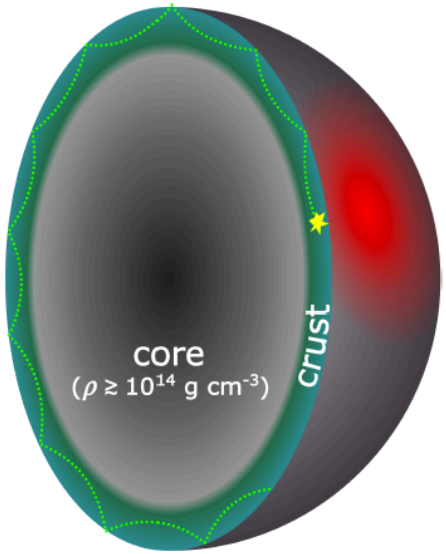

Ejecta Model

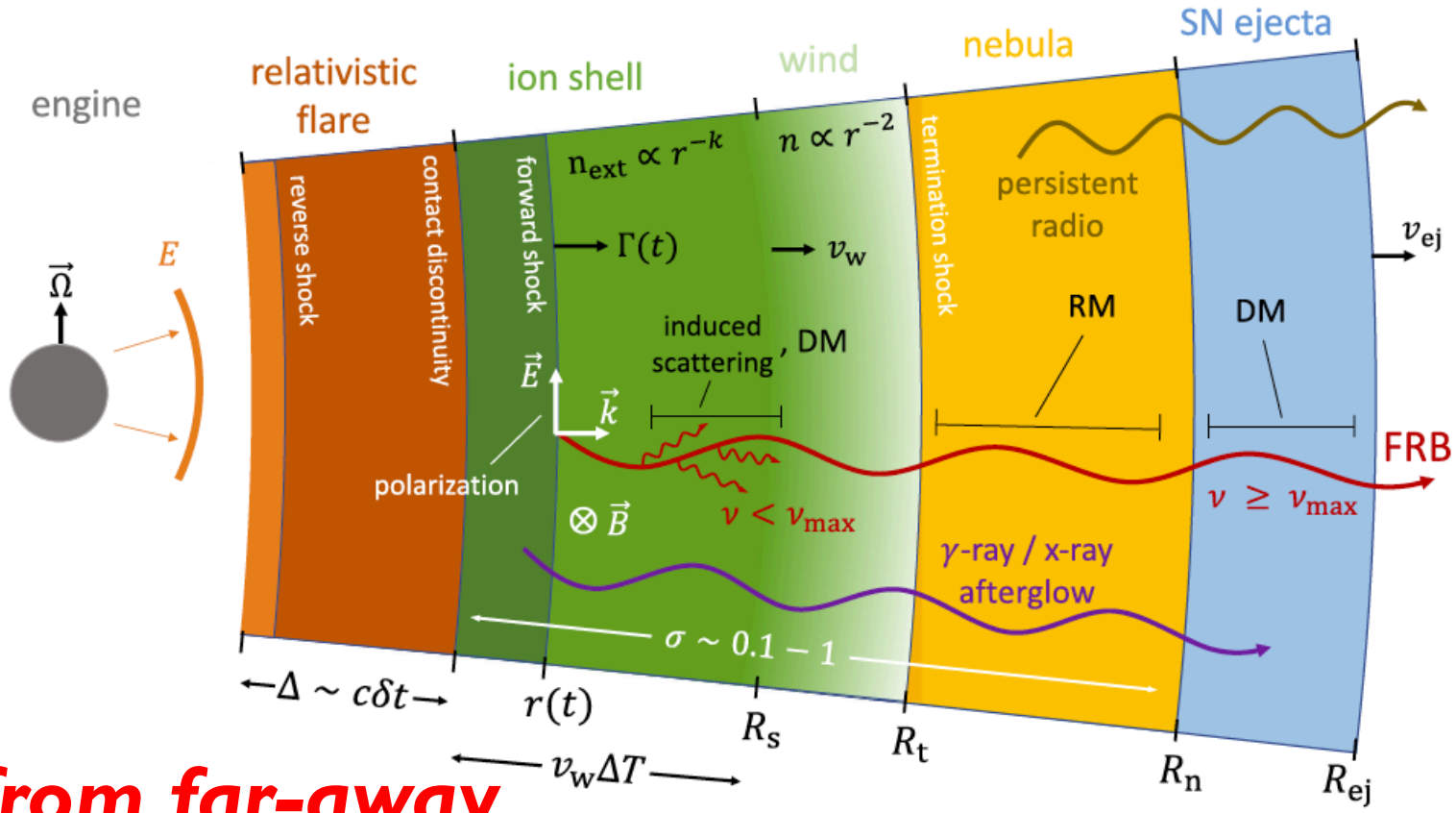

FRB from far-away circum-stellar matter interacting with relativistic ejecta

Margalit et al. 2020; Yu et al. 2020; Yuan et al. 2020
Lyubarsky 2014; Murase et al. 2016; Waxman 2017;
Beloborodov 2017; Metzger et al. 2017

Table 1: **Properties of burst from SGR 1935+2154.**

Parameter	Component 1	Component 2
Dispersion measure (pc cm^{-3})	332.7206(9)	
Scattering timescale (ms)[a]	0.759(8)	
Arrival time (UTC, topocentric)[b]	14:34:24.40858(2)	14:34:24.43755(2)
Arrival time (UTC, geocentric)[b,c]	14:34:24.42848(2)	14:34:24.45745(2)
Scattering-corrected width (ms)	0.585(14)	0.335(7)
Spectral index[a,d]	−5.75(11)	3.61(8)
Spectral running[d]	1.0(3)	−19.9(3)
Fluence (kJy ms)	480	220
Peak flux density (kJy)	110	150

Values in parentheses denote statistical uncertainties corresponding to the 68.3% confidence interval in the last digit(s).

[a] Quantities are referenced to 600 MHz.

[b] Listed arrival times were corrected for the frequency-dependent time delay from interstellar dispersion using the listed dispersion measure, and are referenced to infinite frequency.

[c] Arrival times at the geocenter were obtained after correcting the listed topocentric times for the geometric delay, assuming an ICRS source position of (R. A., Dec.) = ($19^h34^m55.606^s$, 21°53′47.4″)[13], and an observatory position of (Long., Lat.,Height)$_{\rm CHIME}$ = (119°36′26″ W, 49°19′16″ N, 545 m.).

[d] Quantity defined in Methods.

CHIME+ 2005.10324

Table 1: **Data on ST 200428A.** Standard errors in the final significant figures (68% confidence) given in parentheses.
[a] The correction to the infinite-frequency ($\nu = \infty$) arrival time is done using the DM quoted in this table, and assuming a dispersion constant of $\frac{1}{2.41} \times 10^4\,\mathrm{s\,MHz^2\,pc^{-1}\,cm^3}$ [14].
[b] The full-width half-maximum (FWHM) of the Gaussian used to model the intrinsic burst structure (Methods).
[c] This assumes a distance to SGR 1935+2154 of 9.5 kpc.

Property	**Measurement**
OVRO arrival time at $\nu = 1529.267578\,\mathrm{MHz}$ (UTC)	28 April 2020 14:34:25.02657(2)
OVRO arrival time at $\nu = \infty$[a] (UTC)	28 April 2020 14:34:24.43627(3)
Earth centre arrival time at $\nu = \infty$[a] (UTC)	28 April 2020 14:34:24.45548(3)
Fluence (MJy ms)	1.5(3)
Dispersion measure ($\mathrm{pc\,cm^{-3}}$)	332.702(8)
Intrinsic burst FWHM[b] (ms)	0.61(9)
Isotropic-equivalent energy release[c] (erg)	$2.2(4) \times 10^{35}$

scattering ~0.4(1) ms@1GHz

T_b~1.4e32 K

No evidence for a local DM

Bochenek+ 2005.10828

No Detection by FAST

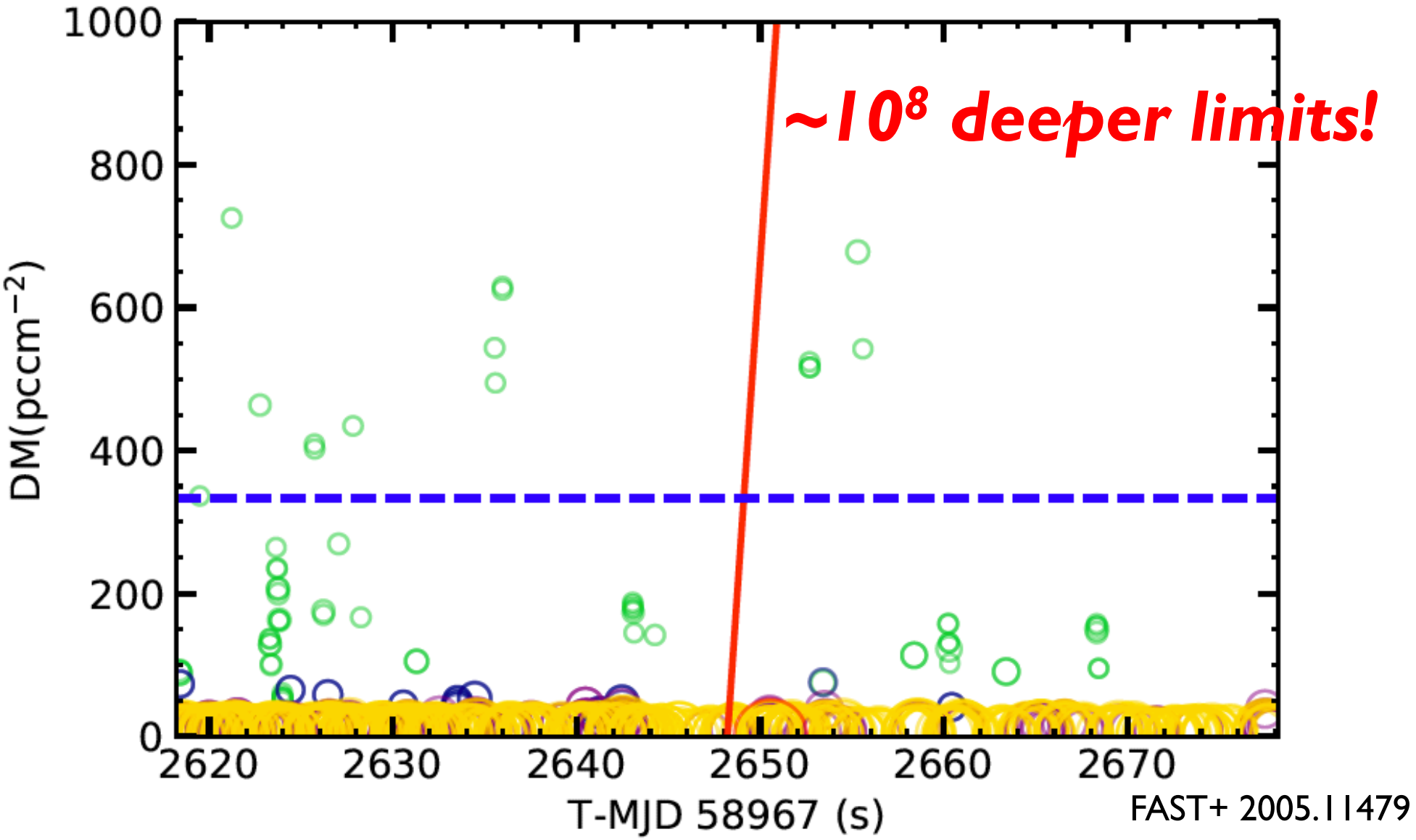

FAST+ 2005.11479